

True Zero Emission Electric Aircraft Propulsion Transport Technology

Rodger W. Dyson¹

NASA Glenn Research Center, Cleveland, OH, 44135, USA

This work establishes and describes a new electric aircraft propulsion technology category for achieving true zero greenhouse gas emission with transport aircraft. This new category is enabled by a recently invented Closed Strayton Quad Generator and recently developed megawatt-scale electric propulsor motors that enable staged contra-rotating ducted fans in a single nacelle. After a brief review of the existing state of practice, a new electric aircraft propulsion system is described that is quiet, clean, efficient, reliable, safe and supports the global transition from jet fuel and sustainable aviation fuel to future green hydrogen fuel with the goal of achieving truly zero impact on the environment. A proposed design of this propulsion system is presented along with a performance and mass comparison to current state of practice.

I. Nomenclature

\dot{W}	= power output
\dot{W}'	= specific power output
\dot{m}_c	= mass flow through compressor
\dot{m}_e	= mass flow through expander
\dot{m}_b	= mass flow through burner
\bar{C}_{pc}	= mean specific heat during compression
\bar{C}_{pe}	= mean specific heat during expansion
\bar{C}_{pb}	= mean specific heat during heat addition
η_{pc}	= compressor polytropic efficiency
η_{pe}	= expander polytropic efficiency
η_{th}	= cycle thermal efficiency
ϵ_x	= recuperator heat exchanger effectiveness
T_{01}	= Total temperature compressor inlet
T_{02}	= Total temperature compressor outlet
T_{03}	= Total temperature heater inlet
T_{04}	= Total temperature turbine inlet
T_{05}	= Total temperature turbine outlet
p_0	= Total pressure
Δp_0	= Total pressure changes in component
r	= Total pressure ratio across compressor
T'	= Temperature ratio of Brayton cycle

II. Introduction

The U.S. aviation sector has been challenged to achieve net-zero emissions by 2050 [1]. Among all aircraft types, the narrow body and wide body aircrafts are associated with 93% of the aviation CO₂ emissions [2]. Hence, this paper focuses on large transport aircraft for the greatest aviation emissions reduction. When comparing all the aviation emissions' impact on the environment, carbon dioxide (CO₂) accounts for 33% on average, while non-CO₂

¹ Power and Propulsion Technical Lead, Thermal Energy Conversion Branch.

contributes to around 67%, including nitrogen oxides (NO_x) and contrails [3]. Numerous recent technology gap and review papers have identified the importance and challenges of achieving a true zero greenhouse gas emission (GHG) transport aircraft. As shown in Figure 1, there are five overall categories for reducing GHG emissions ranging from more electric, SAF, hybrid electric, hydrogen combustion, and ultimately fuel cell or battery electric for achieving true zero GHG [4-11]. The focus of this paper is the creation of a new true zero GHG technology category called Closed Strayton as shown in the bottom right of this figure.

The environmental impact and limitation of each fuel type and technology used are also highlighted in Table 1.

Note that fuel cells are currently the best true zero GHG emission technology but due their mass it is challenging to utilize conventional tube-and-wing configurations. Moreover, PEM fuel cells have a limit life of about 10,000 h and require inlet air compression and humidification at high altitudes resulting in complex and heavy balance of plant. Hydrogen turbofans are the next likely option for transport class vehicles and are being pursued by industry presently. However, they present several challenges including hydrogen turbine embrittlement, multiphase cryopump complexity, and still produce GHG and noise. SAF is attractive to industry because operations largely remain unchanged, but SAF still produces GHG and as shown in Table 2 requires more energy to produce than green hydrogen. Battery technology is simply too heavy for transport class aviation. Hybrid electric offers between 3-5% fuel burn reduction in transport class aircraft, but fundamentally contributes significant GHG emissions. The Closed Strayton Quad Generator, which is the topic of this paper, is a new true zero GHG technology that can achieve a maximum overall net climate impact for transport class aircraft [34-38].

As shown in Table 2, only jet fuel can be considered a positive net energy source. Batteries, green hydrogen, and SAF require an external energy source to charge or create it. But only green hydrogen has the potential to enable true zero GHG transport if the limitations of batteries and fuel cells can be avoided.

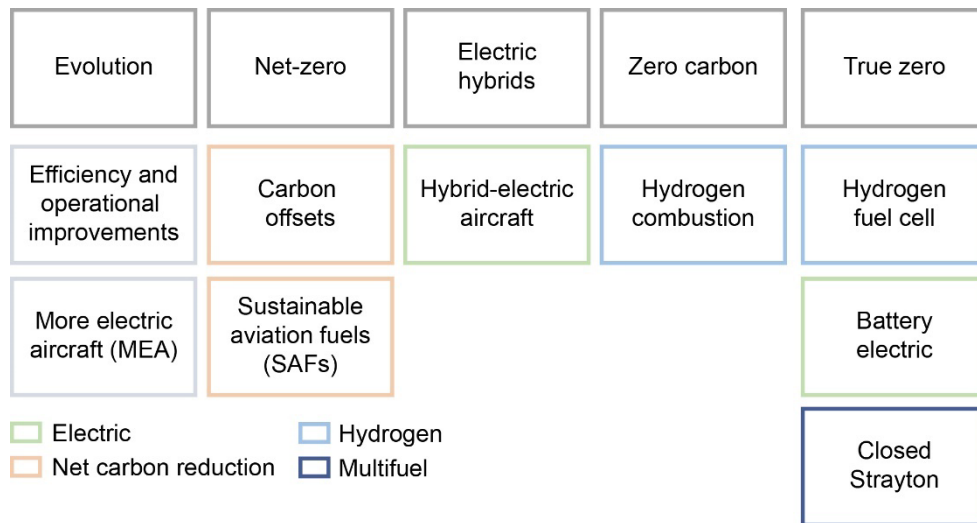


Fig. 1. New Category for True Zero Greenhouse Gas Emission Transport Aircraft

Table 1.

Propulsion power sources	(Emission reduction) × Scalability × Specific power = Net impact					
	CO ₂	NO _x	Contrail	Scalability	Specific power	Net impact
H ₂ fuel cell	Green	Green	Green	Green	Yellow	Yellow
H ₂ combustion	Green	Red	Red	Green	Green	Yellow
Sustainable fuel	Yellow	Red	Red	Green	Green	Red
Battery electric	Green	Green	Green	Red	Red	Red
Hybrid electric	Yellow	Red	Red	Yellow	Yellow	Red
	Green	Good	Yellow	Moderate	Red	Limited

Table 2.

Energy type	Energy required to produce 1 MJ	Cost per MJ (\$)	Availability	GHG pollution
Kerosene jet fuel	0.19	0.03	Limited to ~100 years	CO ₂ , NO _x , soot, contrails, etc.
Battery	1.09	0.04	Limited rare earth supply	Can be very low with renewables but too heavy
Green hydrogen	1.63	0.06	Unlimited water with solar, wind, nuclear but need infrastructure	NO _x , contrails with combustion, none with lightweight CSG or heavy fuel cells
SAF (SPK)	2.56	0.08	Feedstock scaling challenge	Net zero CO ₂ , but still NO _x and contrails
SAF (PTL)	>2.56	0.10	Most scalable synthetic option	Net zero CO ₂ , but still NO _x and contrails

Specifically, of the various fuel types and technologies employed, only PEM fuel cells and all electric battery powered aircraft can achieve true zero GHG emissions, but they carry significant mass, volume, and life limitations that make them intractable for MW-scale transport aircraft propulsion conventional airframes. So overall, the attempt to reduce emissions has meant some combination of:

- Non-standard airframes to address cryogenic hydrogen and volume constraints (with aerodynamic benefits that are often hard to quantify and highly specific to flight conditions),
- Hydrogen turbofans that potentially challenge the structural life of already stressed turbine blades
- Heavy, life-limited fuel cells with significant thermal management challenges beyond 5 MW
- Turbofan power extraction that is already nearing its maximum safe limits (well below 10 MW)

In contrast to these limitations, the Closed Strayton Quad Generator provides a third approach for achieving True Zero GHG emission in a more lightweight, compact, and long-lived package and it will be the primary topic of this paper [90-95].

III. Hydrogen Turbo-Electric Aircraft

The proposed electric aircraft propulsion system can eliminate not only CO₂ but also NO_x, particulates, and contrails to reduce the total aviation Effective Radiative Forcing (ERF) to essentially zero [12-33]. The Strayton technology separates propulsion into a clean power generation unit and an efficient contra-rotating electric propulsion unit as shown in Fig. 2. This combination allows for both aircraft and flight-regime independent clean propulsion.

This is possible because of two features of this system. First, the separated power generation system can provide post-emission controls since the combustion exhaust is not used for propulsion. Second, the propulsor can incorporate staged electric-motor powered fans in the same nacelle to increase thrust without increasing drag. This latter benefit becomes more significant at higher flight speeds as drag nonlinearly increases. In addition, a contra-rotating propeller is known to boost the propulsion efficiency by ~20% [96-118], but such benefits are typically offset by its mechanical complexity and added weight.

In contrast to these limitations, the recently invented Closed Strayton Quad Generator provides a novel third approach for achieving True Zero GHG emission in a more lightweight, compact, and long-lived package. As shown in Fig. 3 today's turbofans have an overall combined thermodynamic and propulsion efficiency of approximately 40%. This is achieved with a combination of high bypass ratios (>10), high compression ratios (>40), and high temperature ratios (>6). Most of the thrust (>80%) is produced from the low-pressure ratio fan with the balance of the thrust from the nozzle. The combustion occurs in the core of the turbofan and the exhaust exits through the rear nozzle as part of the thrust gases. This architecture, while very efficient and lightweight, presents few opportunities for post emission control.

In contrast, turbogeneration architectures in which all the thrust is provided by electric motor propulsors, the combustion exhaust gases are not used for high velocity thrust. Instead, the relatively low velocity combustion gases travel through what is in essence a muffler. This enables post combustion emission control technologies such as are currently used in diesel trucks. Further, if the turbogeneration uses a closed cycle, it can be pressurized with an inert working fluid for mass reduction. Moreover, the combustion system can be completely separated from the turbomachinery and separately optimized for emissions with both pre- and post- combustion control technologies. The combination of separately optimized combustion, power, and propulsion potentially provides an overall propulsion system efficiency advantage as shown in Fig. 3. If the closed turbogeneration system is small enough at MW-scale it can be installed in the tail-cone of aircraft to generate electric power as shown with electric motor propulsion in the nacelle in this Fig. 4.

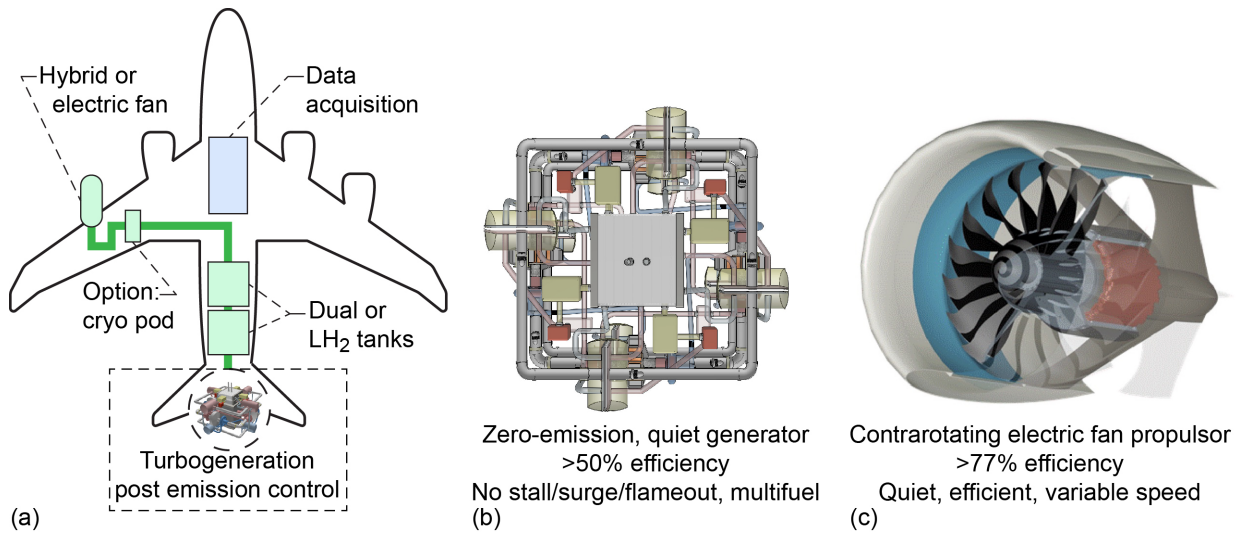


Fig. 2. Separate power and electric propulsion for efficient, quiet, and clean transport vehicle.

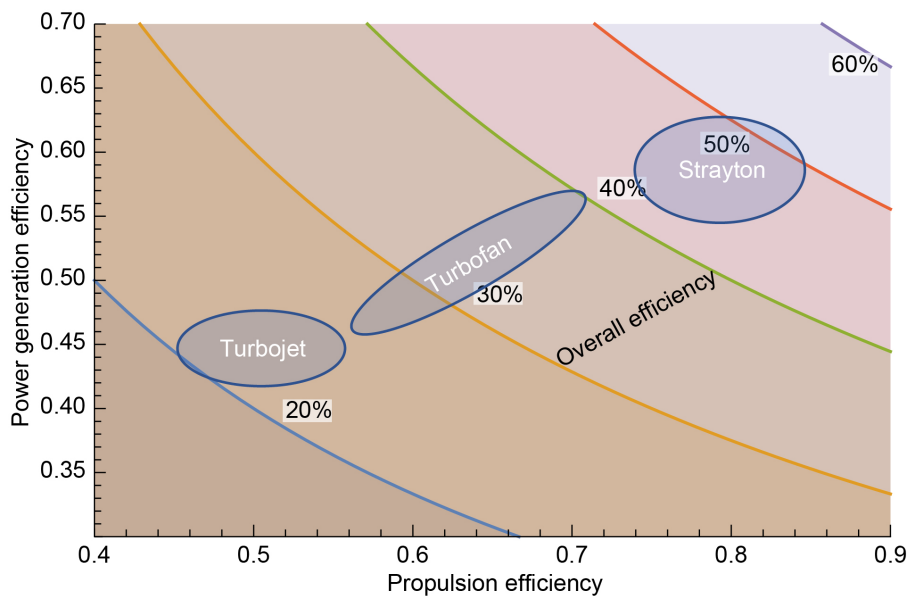


Fig. 3. Separate optimization of power, propulsion, and combustion potentially improves overall efficiency

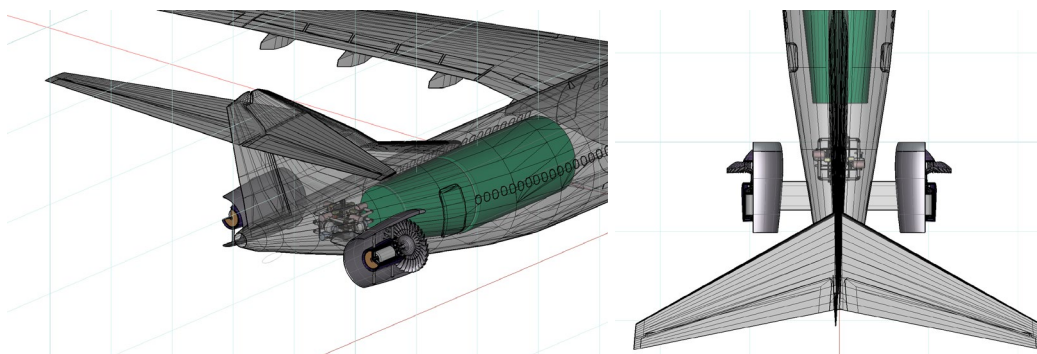


Fig. 4. Closed Strayton Generator and Electric Propulsor Installation

IV. Strayton Fundamentals

The proposed Closed Strayton Quad Generator cycle has an overall higher system efficiency, specific power, and reliability than each individual Brayton and Stirling cycle can achieve separately. The integration is achieved by installing an acoustic Stirling heat exchanger pair in the hollow rotating shaft of a Brayton cycle generator to provide both Brayton turbine conductive cooling and Brayton thermal recuperation as shown in Fig. 5.

The Brayton cycle waste heat acts as a topping cycle delivering thermal energy to the shaft-embedded acoustic Stirling cycle. The four Strayton cycles are combined into a quad configuration to facilitate inter-stage cooling, reheating, and to complete a full acoustic wavelength 360° acoustic loop for significantly increased Stirling power, Brayton internal recuperation, and Brayton turbine cooling as shown in Fig. 6 with single recuperator (top left), inter-cooling (blue arrows), and reheating (red arrows). The purpose of this arrangement is two-fold. First, as shown in Fig. 6, the compressor inter-stage cooling and the turbine inlet reheating at all four stages improves the Brayton cycle efficiency and only requires a single recuperator. Second, the hollow rotating shafts of all four Brayton generators have an acoustic Stirling engine inside [39-47] and the quad configuration enables the four regenerators to be located acoustically $\frac{1}{4}$ wavelength apart. This is like earlier multi-stage Stirling engines that used pistons that oscillated with a 90° phase angle difference as shown in Fig. 7, but instead of using oscillating pistons, we locate each acoustic Stirling engine acoustically 90° apart to achieve the same higher specific power acoustic Stirling cycle without the complication of mechanical linkages as shown in Fig. 8.

The high-power acoustic power loop shown in Fig. 8 provides turbine cooling, Brayton bottoming cycle, combustor bottoming cycle, or inter-cooling bottoming cycle depending on the level as shown in Fig. 9. It also provides acoustic cooling power for other powertrain components.

The full Closed Strayton quad configuration has three levels with a single recuperator as shown in Fig. 9.

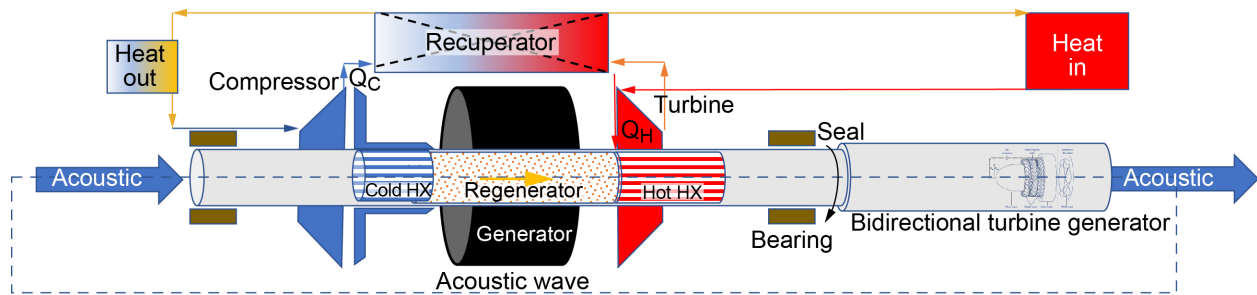


Fig. 5. Strayton Generator Fundamentals

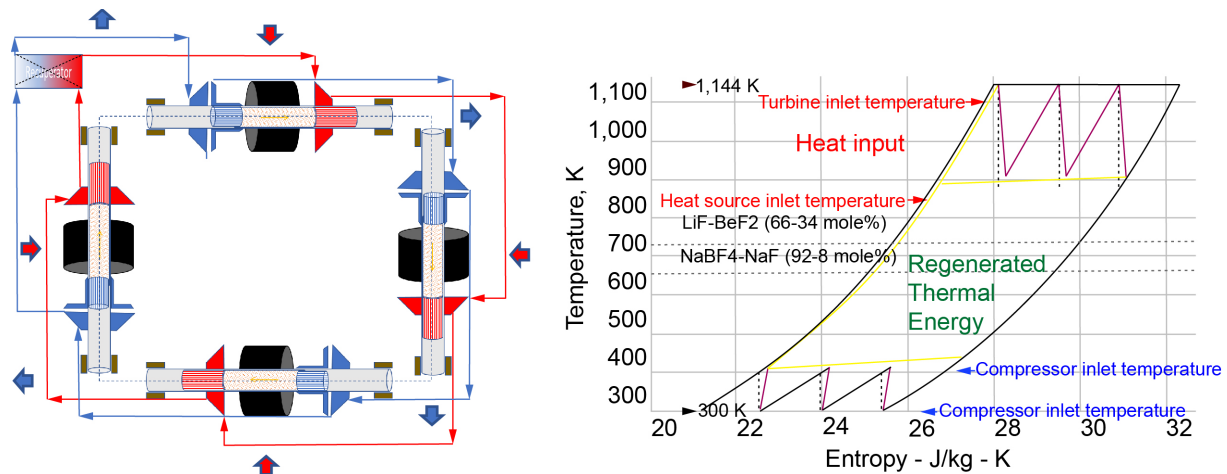


Fig. 6. Strayton Generator Quad Configuration with Acoustic Inter-Cooling and Reheating

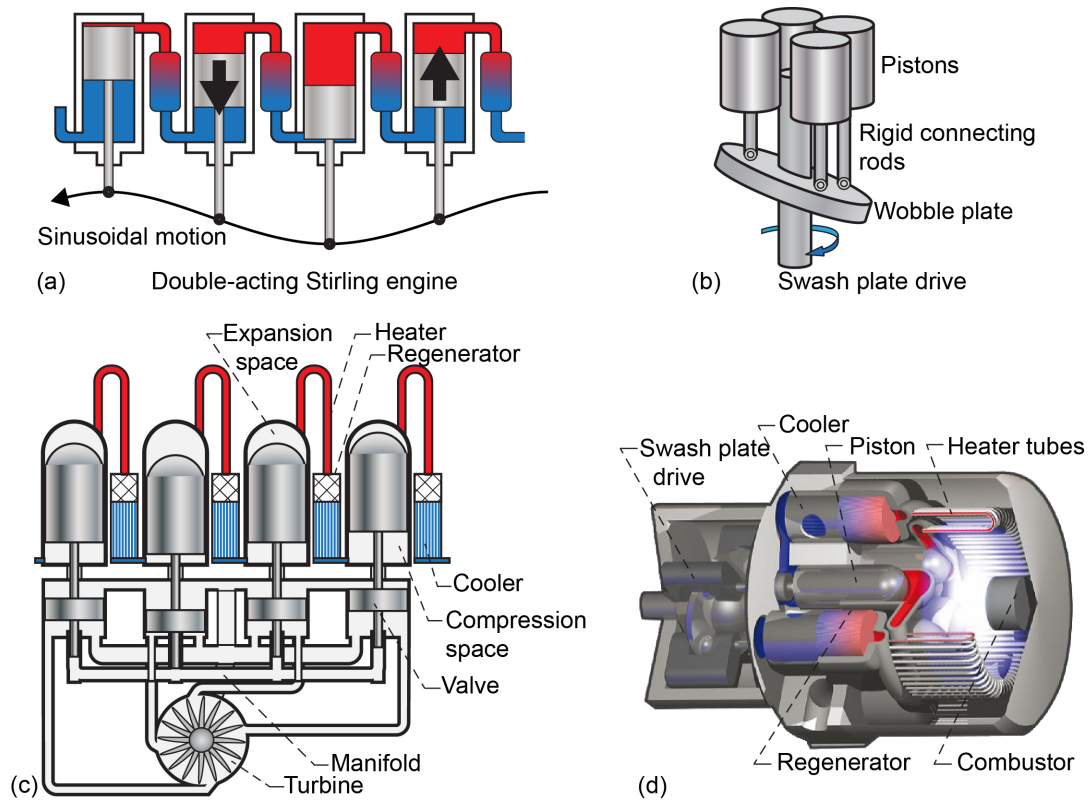


Fig. 7. Multistage Stirling Engines

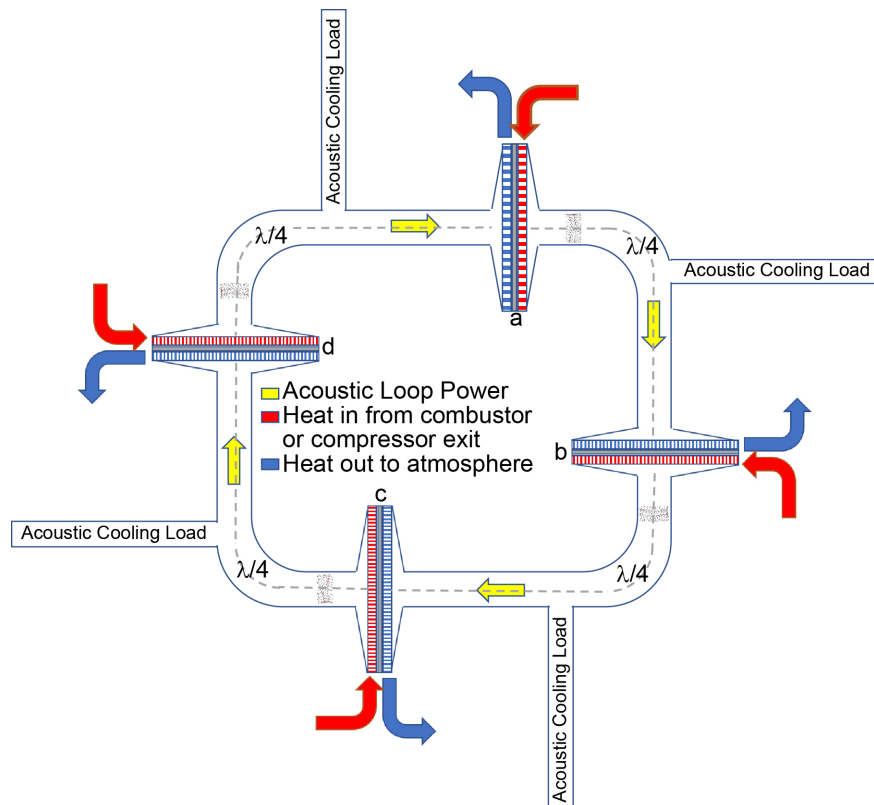


Fig. 8. Multistage Acoustic Stirling Engines (no mechanical linkages)

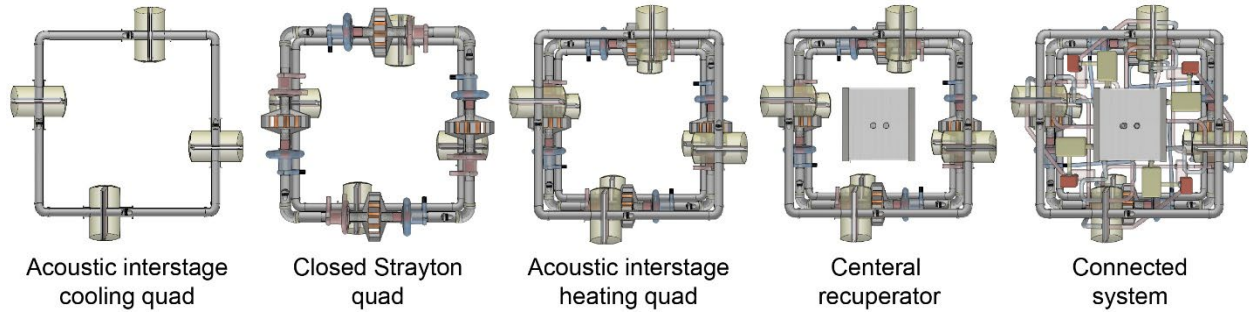


Fig. 9. Three Layers: Acoustic Inter-cooling, Strayton, and Acoustic Reheating

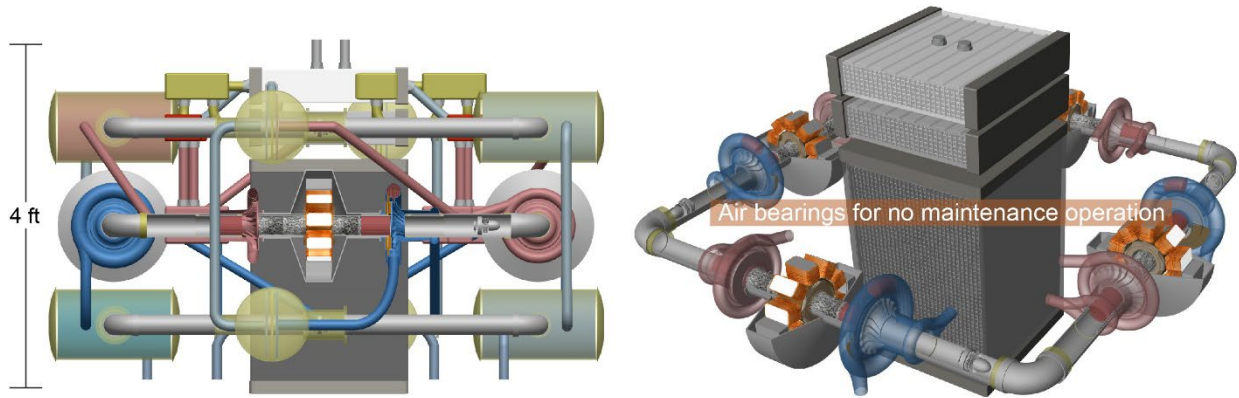


Fig. 10. MW-scale Zero-Emission Closed Strayton Quad Generator

Each quad layer has an acoustic Stirling loop with four no moving part acoustic engines and the middle layer also has the four rotating Brayton engines. In total, we have 16 engines combined synergistically. The only moving parts are the four Brayton shafts and the 3 bi-directional turbine acoustic generators. The moving parts are supported by no-contact gas bearings that do not require maintenance or have a life limiting mechanism. In summary, a new compact zero-emission Closed Strayton Quad Generator system is shown in Fig. 10.

Due to its hermetically sealed working fluid, it is aircraft-type and flight-speed independent since the working fluid is pressurized and is environment independent. It also allows the post-combustion emissions to be fully managed to provide essentially zero greenhouse gas emission since exhaust gases are routed through a low-speed muffler instead of being directly inserted into the jet for propulsion.

V. Zero-Emission Closed Strayton Quad Generator

Since the Closed Strayton Quad Generator separates the combustion from the turbine exhaust, it can be optimized to provide true zero GHG emissions by utilizing a combination of the following three mechanisms:

- Pre-combustion steam input from either fuel cell exhaust or hydrogen combustion steam recirculation
- Post-combustion emission control within the muffler exhaust tube
- Operating the combustor at a lower temperature to avoid NO_x production

As shown in Fig. 11, the exhaust water vapor can be recuperated with air followed by cryogenic fuel to achieve not only high combustion efficiency but to also control the production of contrails. The sealed working fluid enables the use of pressurized gas bearings for long-life lubrication-free no contact operation. This eliminates the potential for lubrication oils to form particulates that contribute to contrail formation. The steam mixer in Fig. 11 can be replaced with a fuel cell to act as a topping cycle for the Closed Strayton cycle while also producing steam, adding heat to the combustor, and generating DC electric power. Since it is primarily used for water generation it can be kept small relative to the overall system. It should be noted that in Fig. 11 the quad configuration is assumed but is more easily represented as a single Strayton and combustor combination. More examples of variants of this configuration can be found in the appendix.

Table 3.

Fuel	Fuel cell or Exhaust Steam Recirculation	Emissions			
		CO ₂	NO _x	Soot	Contrails
Hydrogen	PEM	Green	Green	Green	Green
Hydrogen	Recirculation	Green	Green	Green	Green
SAF	SOFC	Yellow	Yellow	Yellow	Yellow
A1	SOFC	Red	Yellow	Red	Red

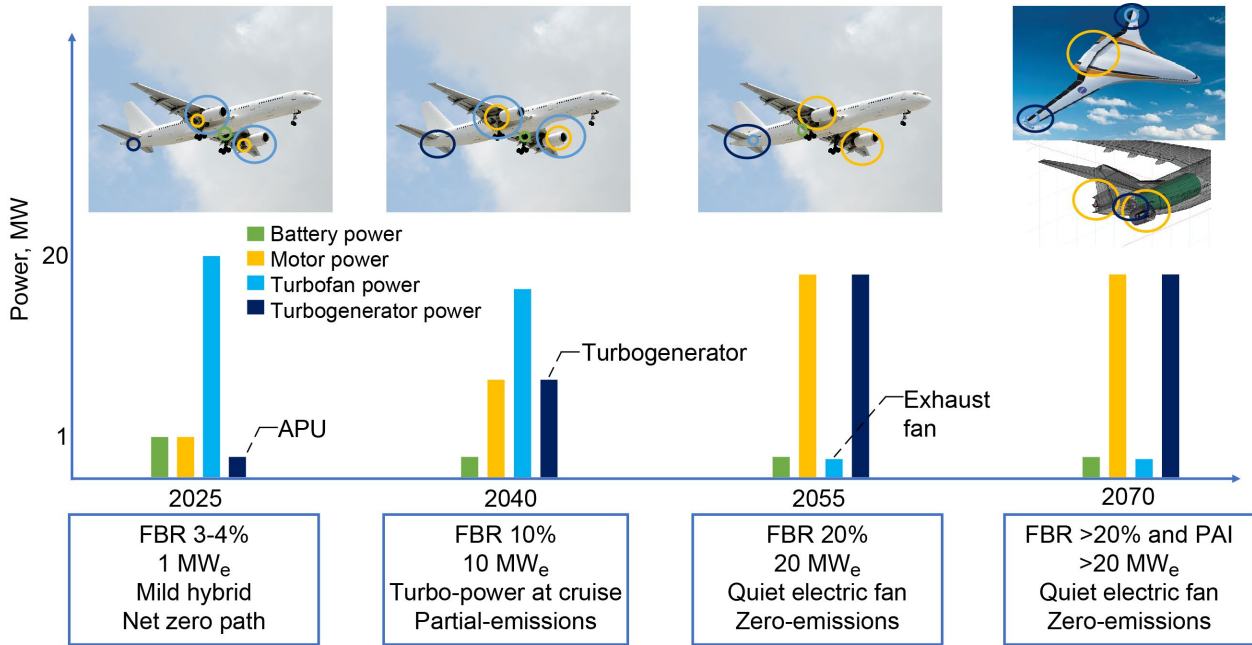


Fig. 12. Closed Strayton Generator Enables SAF and Hydrogen Dual Fuel Transition and Electric Motor Propulsors on Aircraft

A key point is that electric aircraft with a Closed Strayton Quad Generator enables the gradual transition of dual fuel aircraft without requiring complicated propulsion airframe integration to achieve a net propulsive and climate benefit. As shown in Fig. 12, eventually additional benefits can be derived with advanced airframes. It should be noted that because both SAF and hydrogen fuel require more energy to produce than they can store as listed in Table 2, it will be important to find additional ways to reduce aircraft drag using advanced airframes because for example a 1% fuel savings on the aircraft will result in ~2% energy savings overall.

Another key point is that since hydrogen fuel can provide true zero emissions with this technology, then a dual fueled vehicle with 10% clean power and 90% conventional fuel will see a 10% drop in emissions compared to a 100% conventional fueled vehicle. It is likely easier in the near term to focus on dual fuel emission reduction than to achieve a 10% reduction in fuel burn with electric aircraft technology alone. In other words, the potentially best use of electric aircraft technology is emission reduction with dual fuels instead of conventional fuel burn reduction.

VI. Closed Strayton Quad Generator Technical Details

Following the previous brief introduction in what the Closed Strayton Quad Generator is and does, this section will explain in greater detail both the physics and thermodynamics of this new technology. In addition, estimates of specific work, specific heat, and cycle efficiency over a range of operating conditions are presented.

A. Basic Architecture

A new thermal energy conversion power generation technology is presented that combines the historically higher power Brayton and lower power Stirling cycles into a new Strayton Quad cycle that has an overall higher system efficiency, specific power, and reliability than each individual cycle can achieve independently. The integration is achieved by installing an acoustic Stirling heat exchanger pair in the hollow shaft of a rotating Brayton cycle generator to provide both Brayton turbine conductive cooling and Brayton thermal recuperation. The Brayton cycle waste heat acts as a topping cycle delivering thermal energy to the shaft-embedded acoustic Stirling cycle. The four Strayton cycles are combined into a quad configuration to facilitate inter-stage cooling, reheating, and to complete a full acoustic wavelength multi-phase loop for significantly increased Stirling power, Brayton internal recuperation, and Brayton turbine cooling. The Brayton specific power and efficiency increases due to the higher allowable turbine inlet temperatures; quad configuration with inter-stage cooling and reheating; and a higher rotational speed when combined with a switched reluctance generator. The shaft-embedded acoustic Stirling specific power increases due to the quad self-amplifying acoustic loop configuration and the high power bi-directional acoustic turbine generators. The recuperator and heat exchanger masses are further reduced with two additional quad loops that provide Brayton stage inter-cooling and reheating with acoustic Stirling topping and bottoming cycles. The reliability increases because the system still operates even under multiple fault conditions, has no-contact seals and bearings, and can safely operate at much higher generator and fluid temperatures without exotic materials. The only moving parts are the rotating Strayton shafts and the rotating bi-directional acoustic turbine generators, which use pressurized gas bearings for long-lasting no maintenance operation. It specifically enables a new class of zero emission electric aircraft propulsion and a reliable higher system alpha electric spacecraft propulsion system. In addition, this technology provides the nascent terrestrial small modular nuclear power generation market with a higher efficiency fault-tolerant generator option.

B. Theory

In the Strayton engine cycle, the Brayton and Stirling cycles operate in synergy, with the Stirling thermoacoustic cycle acting as a recuperator for the Brayton cycle and the Brayton cycle acting to power the Stirling. The architecture of this engine consists of a gas turbine engine, with an alpha thermoacoustic heat exchanger pair installed inside the hollow rotating turbomachinery shaft as shown in Fig. 5. Heat transfer rate, \dot{Q}_H , is drawn down through the turbine blades and is used to power the acoustic Stirling engine. Wasted thermal power, \dot{Q}_C , from the acoustic Stirling cycle is then introduced to the gas turbine system using a heat exchanger directly before engine combustion through the thrust bearing that is paired with an oscillating heat pipe heat exchanger.

This architecture has two main advantages. First, pulling heat down through the turbine blades has a cooling effect on the structure allowing the system to reduce or remove blade cooling flow. Second, acoustic Stirling waste heat is used to create a recuperation cycle within the gas turbine, increasing overall Brayton efficiency. Electric power from the system is delivered via two mechanisms, a Brayton shaft rotation generator, and a separate acoustic bi-directional turbine generator located outside the rotating shaft.

A few key points to note are that the rotating Brayton shaft is separated from the non-rotating structures with a clearance seal that is hermetically sealed from the environment but intentionally has a leakage path between the Brayton and Stirling cycles, so they effectively share the same pressurized working fluid.

The possible working fluid choices are quite varied, but the best system performance is expected with He-Xe for non-economic high-performance applications and He-N₂ for commercial applications as shown in Fig. 13.

The pressurized working fluid in a Closed Strayton generator increases the specific power by reducing the turbomachinery size, by increasing the rotational speed which reduces the switched reluctance generator size, and by increasing the bi-directional turbine efficiency as shown in Fig. 14. Note that the same pressurized high molecular weight working fluid benefits both the Brayton and Stirling cycles but for different reasons; For Brayton, it reduces the size of the turbomachinery and generator by increasing the rotation speed; For Stirling, it increases the acoustic bi-directional turbine efficiency. This unique property is one reason Strayton has a higher overall better performance.

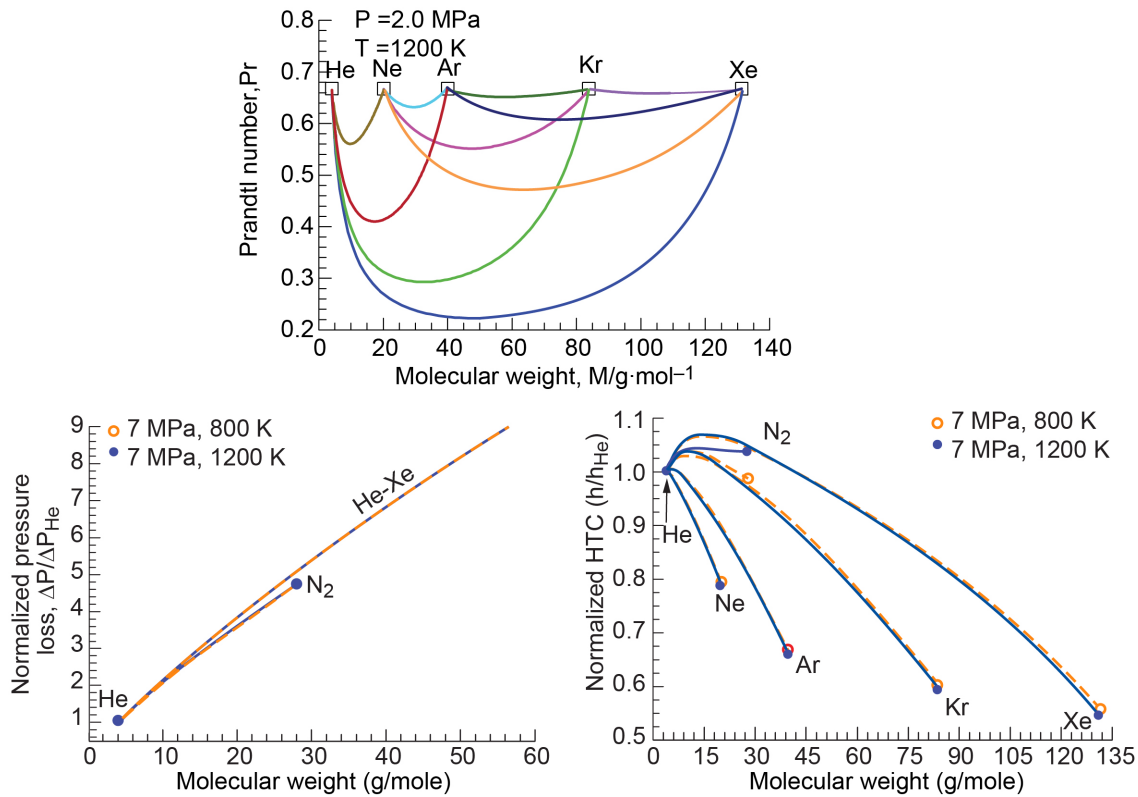


Fig. 13. Working Fluid Optimization

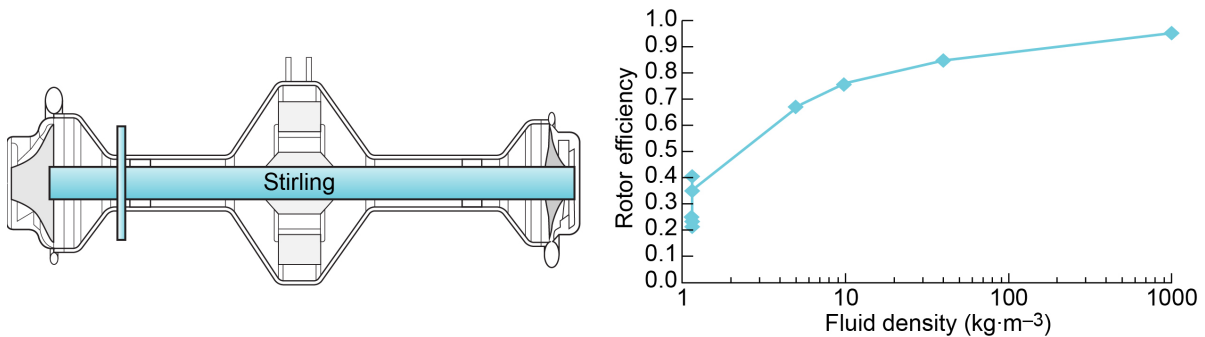


Fig. 14. Pressurized fluid reduces turbomachinery and generator size while increasing acoustic generator efficiency

C. Brayton Cycle

The Brayton thermodynamic cycle is commonly used in a variety of applications including aircraft turbofan propulsion, terrestrial power generation, and space power generation because it can scale to large power levels. As shown in Fig. 15, the Brayton cycle can be recuperated or non-recuperated and can be open cycle (invented in 1872) or closed cycle (invented in 1938).

As shown in Fig. 16, normally the Brayton cycle efficiency increases as the compressor pressure ratio increases but for a given temperature ratio the specific power begins to decrease with additional pressure ratio growth. This is because the turbine temperature limits prevent the addition of more thermal energy.

If the turbine blade can be cooled, we can achieve both higher efficiency and higher specific power. Historically, as shown in Fig. 17, open cycle Brayton has out-performed closed cycle Brayton because of the difficulty of cooling the turbine blade and the additional mass of heat exchanger recuperation. Fig. 18 shows most of the turbofan improvement is enabled with advanced turbine blade cooling technology. Closed Brayton Quad Generation is expected to follow similar performance improvement trends due to the acoustic blade cooling techniques described previously and because the closed pressurized cycle reduces the size of the turbomachinery that is necessary for effective acoustic conductive cooling at the turbine shaft base.

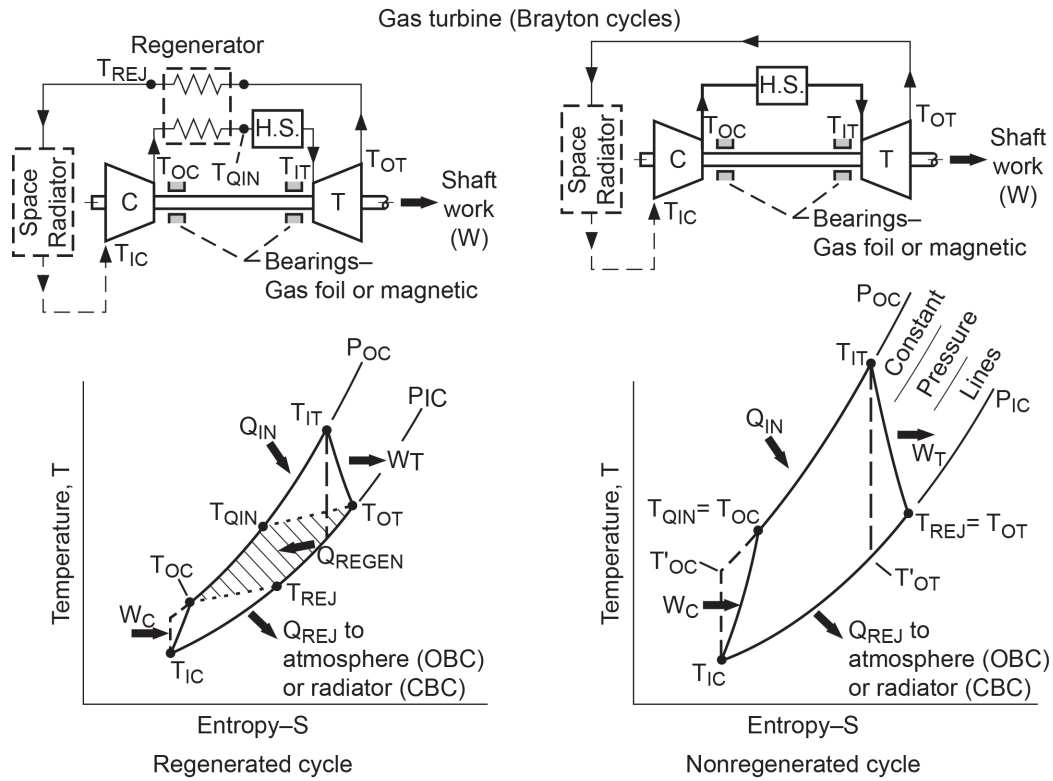


Fig. 15. Open, Closed, Recuperated Brayton Cycles

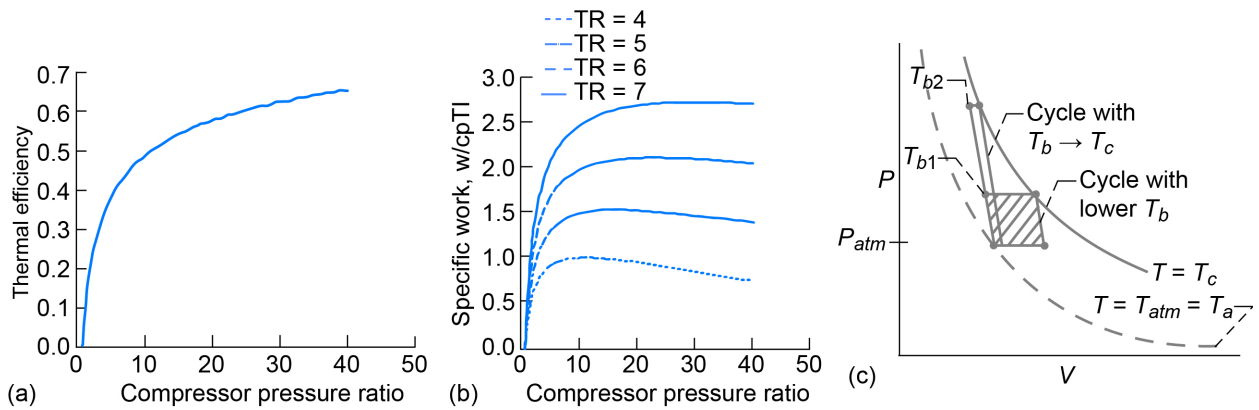


Fig. 16. Brayton Compression Limits at various temperature ratios (TR)

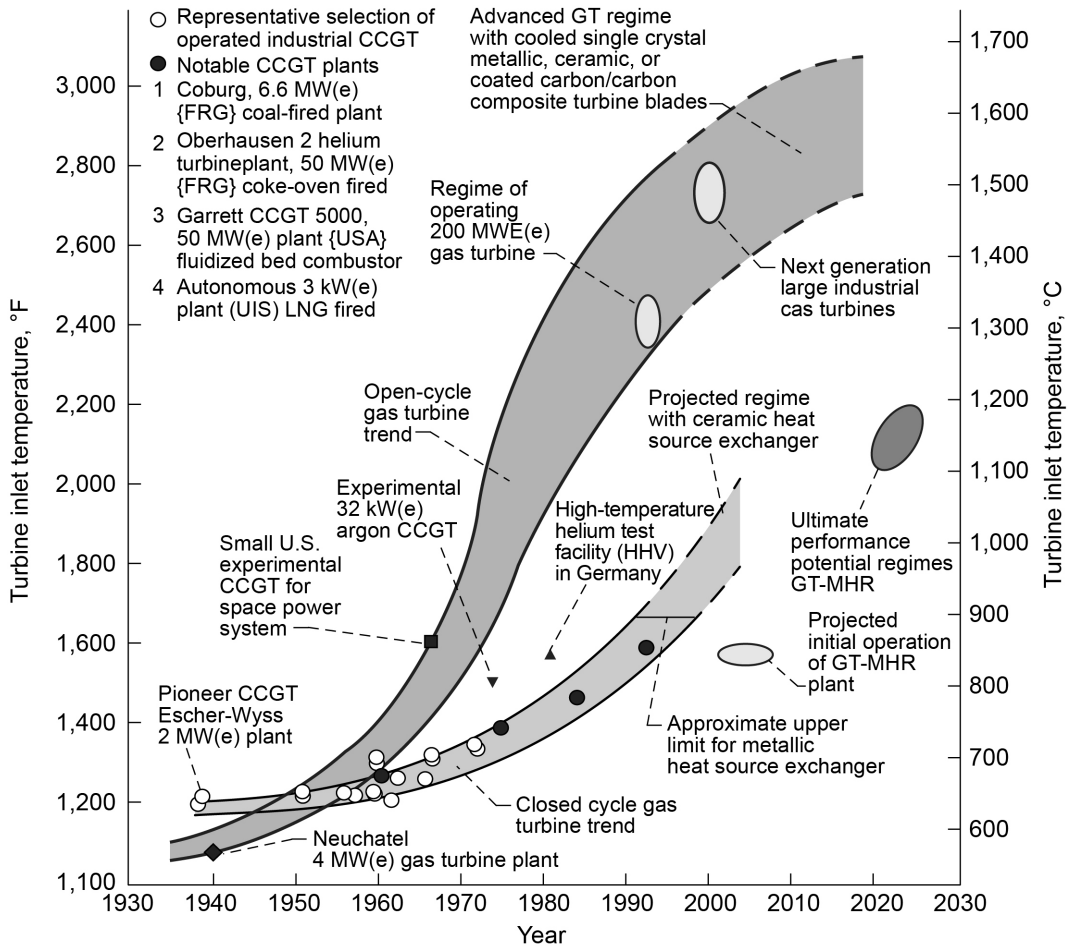


Fig. 17. Historical limitation of Closed Brayton Turbine Inlet Temperature

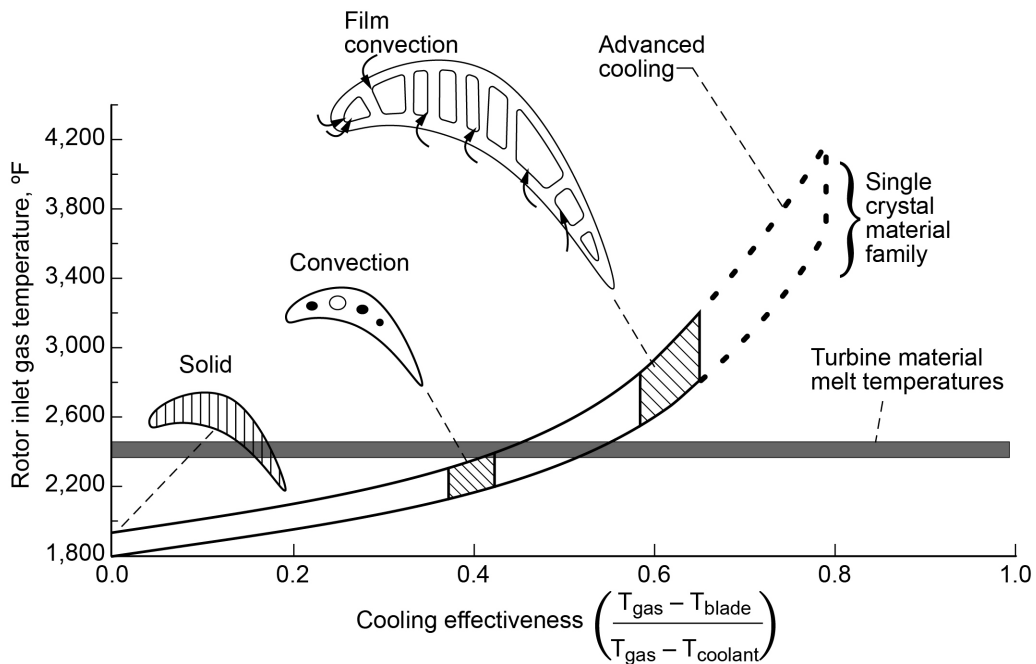


Fig. 18. Closed and Open Brayton Cycle Turbine Temperature Trends

Closed cycle Brayton efficiency is a function of compressor pressure and temperature ratio, but also of the recuperator mass/effectiveness as shown in Figs. 19 and 20.

Note that ERG and ALFA refer to recuperator effectiveness and temperature ratio respectively. In all cases, a higher turbine inlet temperature reduces system mass and increases both system efficiency and system specific power as shown in Fig. 20. This mass estimated in Fig. 20 is for a proposed space application in which radiation is the only means of rejecting thermal energy. But the principle is the same when rejecting waste heat on aircraft, higher temperatures are generally better thermodynamically and offer overall lower system mass [53-81].

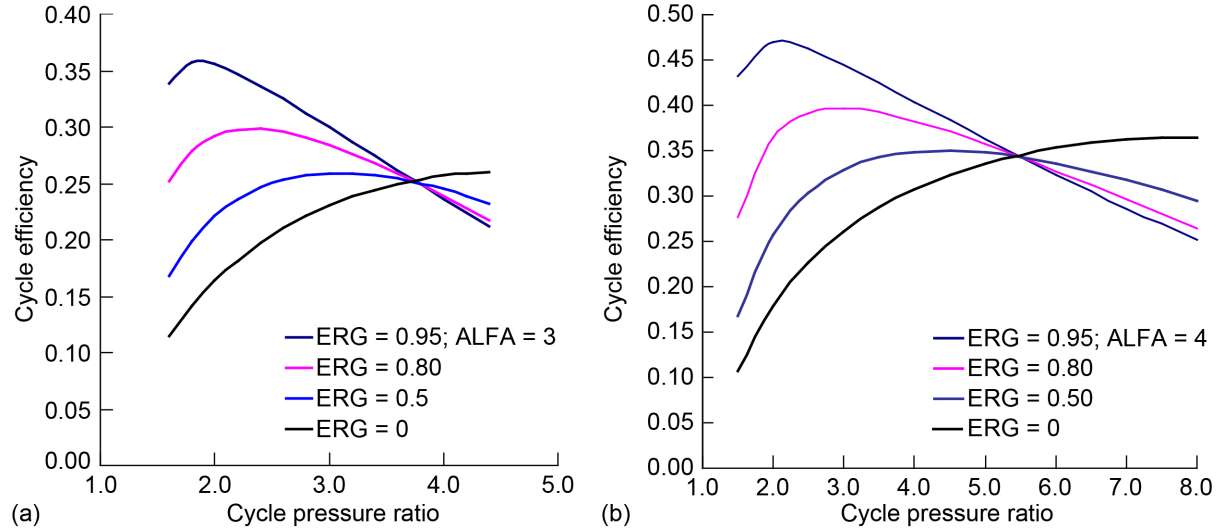


Fig. 19. Closed Brayton Cycle Efficiency. (a) Temperature ratio = 3.0. (b) Temperature ratio = 4.0. (Ref. Juhasz)

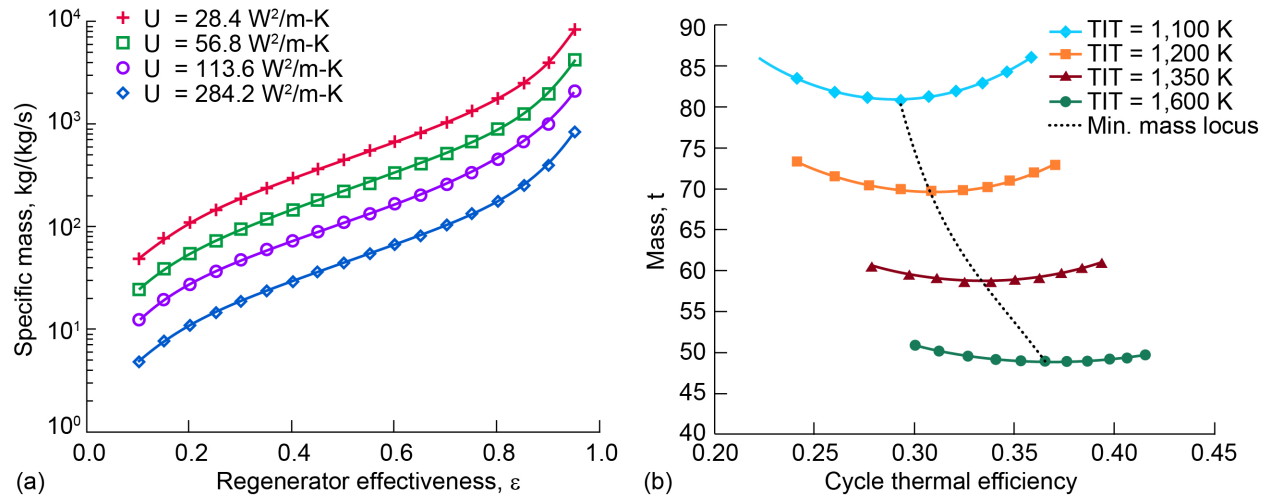


Fig. 20. Specific Mass of Recuperator and System Mass vs. Efficiency (Ref. Juhasz)

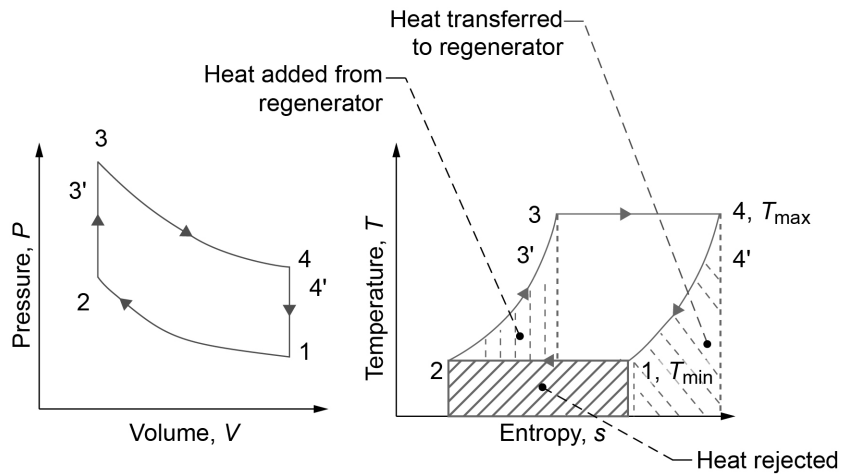


Fig. 21. Closed Stirling Cycle

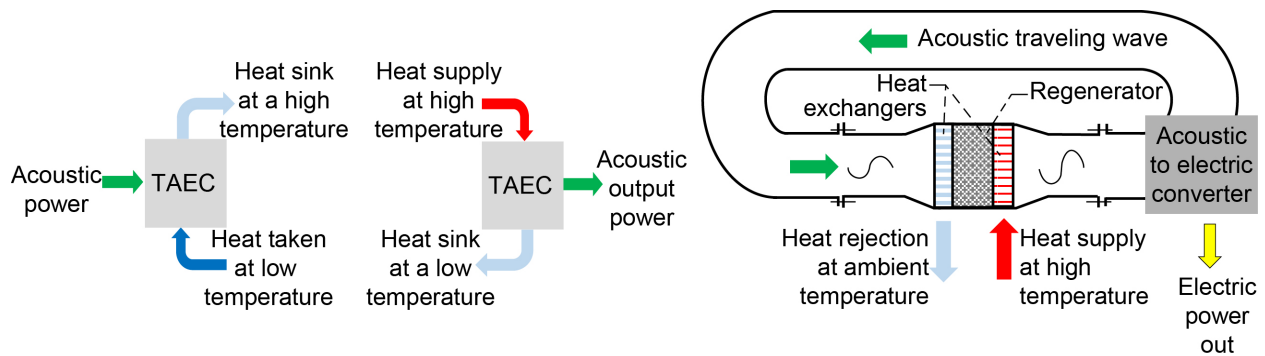


Fig. 22. Acoustic Stirling Fundamentals

D. Stirling Cycle

Similarly, the Stirling cycle shown in Fig. 21 is widely used in lower power applications that require high thermal efficiency. Generally, it is a closed cycle that doesn't scale well to higher power because of oscillating component amplitude and thermal surface heat transfer limits.

1. Acoustic Stirling

The Strayton Quad Generator utilizes a special subset of Stirling engines based on thermoacoustics as shown in Fig. 22. The thermoacoustic Stirling either generates a sound wave with thermal input or it can operate in reverse to provide refrigeration using the energy from an incoming acoustic wave [39-47].

The acoustic wave can generate electric power by either extracting the pressure wave with an oscillating piston, or for higher power levels it can extract the velocity wave with a bi-directional turbine as shown in Fig. 23 [48-52].

As shown in Fig. 24, the acoustic Stirling and piston Stirling have comparable efficiencies, but the acoustic Stirling can operate over a lower range of temperature ratios and higher power levels when combined with a bi-directional turbine generator.

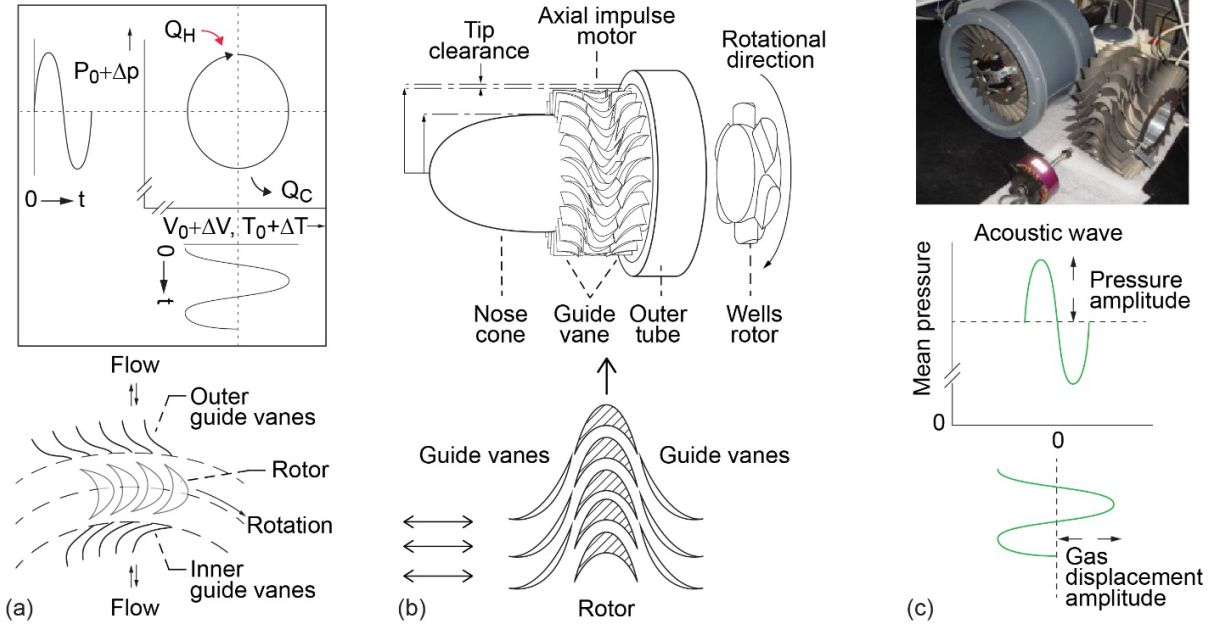


Fig. 23. Bi-directional Turbine Oscillating Velocity Wave Extraction (Ref. Kees de Blok)

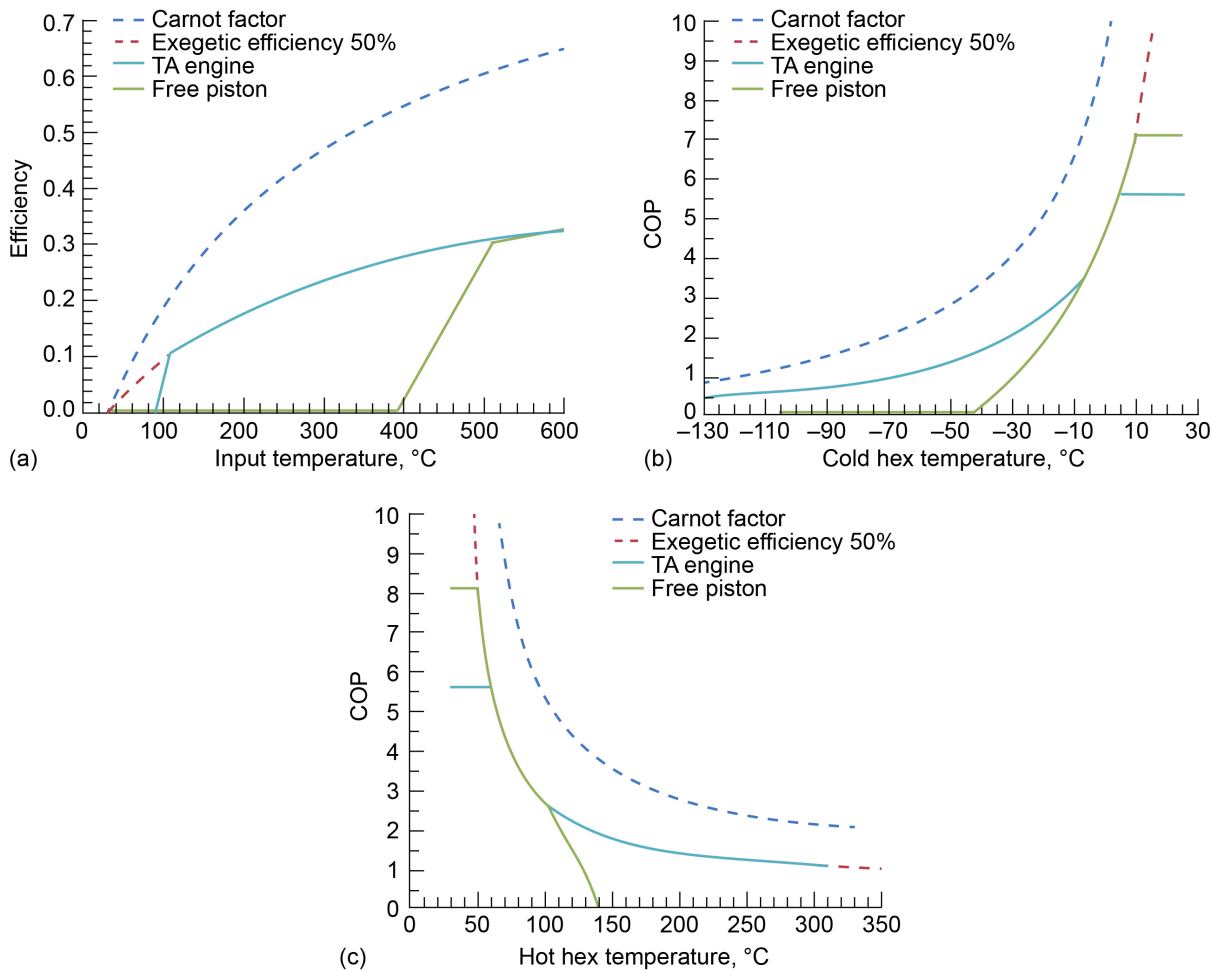


Fig. 24. Acoustic Stirling Engine and Cooler Efficiency (Ref. Kees de Blok)
(a) Thermoacoustic heat engine. (b) Thermoacoustic cooler. (c) Thermoacoustic heat pump.

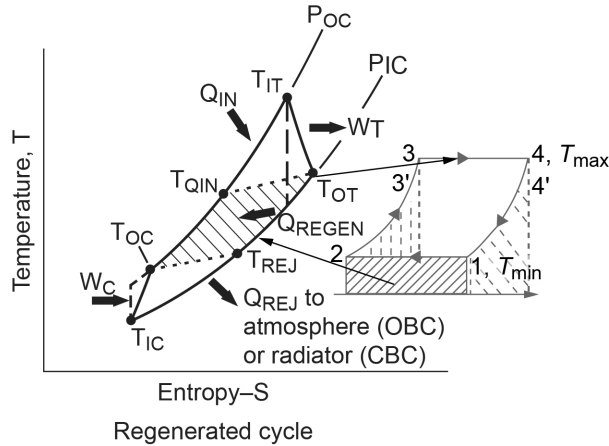


Fig. 25. Open or Closed Recuperated Strayton Cycle

VII. Strayton Cycle

The invention described herein combines the Brayton cycle and acoustic Stirling cycle into a synergistic new Strayton (**Stirling and Brayton**) cycle shown in Fig. 25. Each cycle acts as a topping cycle and bottoming cycle to the other. This is a unique thermodynamic combined cycle property since normally it is not possible to do this. One cycle is normally the topping, and a second cycle is the bottoming (such as gas turbine Brayton topping with steam turbine Rankine bottoming or fuel cell topping with Stirling bottoming) [90-95]. This basic Strayton cycle forms the basic building block for the full quad configuration discussed next.

A. Quad Configuration

A typical Closed Strayton Generator quad configuration is shown in Figs. 6, 9, and 10. It is comprised of four turbo-alternator-compressors connected in a quad loop configuration with a single recuperator (top left), inter-cooling (blue arrows), and reheating (red arrows). The purpose of this arrangement is two-fold. First, as shown in Fig. 6, the compressor inter-stage cooling and the turbine inlet reheating at all four stages improves the Brayton cycle efficiency and only requires a single recuperator. Note a three-stage system T-S diagram is shown in Fig. 6, but the extension to four stages is clear. A detailed four-stage analysis will be presented later.

Second, the hollow rotating shafts of all four Brayton generators have an acoustic Stirling engine inside and the quad configuration enables the four regenerators to be located acoustically $\frac{1}{4}$ wavelength apart. This is like earlier multi-stage Stirling engines that used pistons that oscillated with a 90° phase angle difference as shown in Fig. 7, but instead of using oscillating pistons, we locate each acoustic Stirling engine acoustically 90° apart to achieve the same higher specific power Stirling cycle without the complication of mechanical linkages as shown in Fig. 8.

In addition, the heat exchangers can be replaced with acoustic heat exchangers as shown in Fig. 26. Each heat exchanger has a hot and cold side separated by a regenerator. A portion of the hot input energy is converted to an acoustic wave and the remaining is transferred to the cold side acoustically. Four of these acoustic heat exchangers are placed $\frac{1}{4}$ wavelength apart to form a self-amplifying acoustic loop. The acoustic energy in the loop can be used to generate electricity with a bi-directional turbine generator and/or it can be used to provide cooling of the Brayton generator, power electronics, and other components.

The full quad configuration has three levels as shown in Figs. 10 and 27. Each layer has an acoustic Stirling loop with four no moving part acoustic engines separated by 90° and the middle layer also has the four rotating Brayton engines. In total, we have 16 engines combined synergistically. The only moving parts are the four Brayton shafts and the 3 bi-directional turbine acoustic generators. It is possible to reduce the moving parts to two (one Brayton shaft and one acoustic generator) by some of the configurations shown later in this document. However, the moving parts are supported by no-contact gas bearings that do not require maintenance nor have a life limiting mechanism.

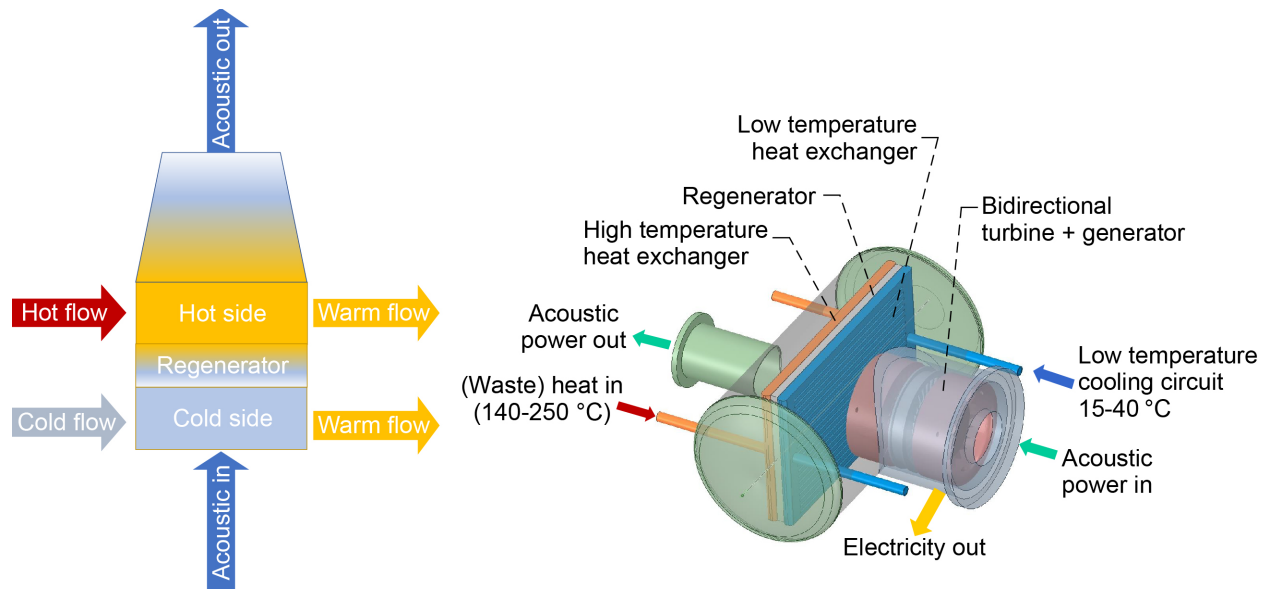


Fig. 26. Acoustic Heat Exchangers (Ref. Kees de Blok)

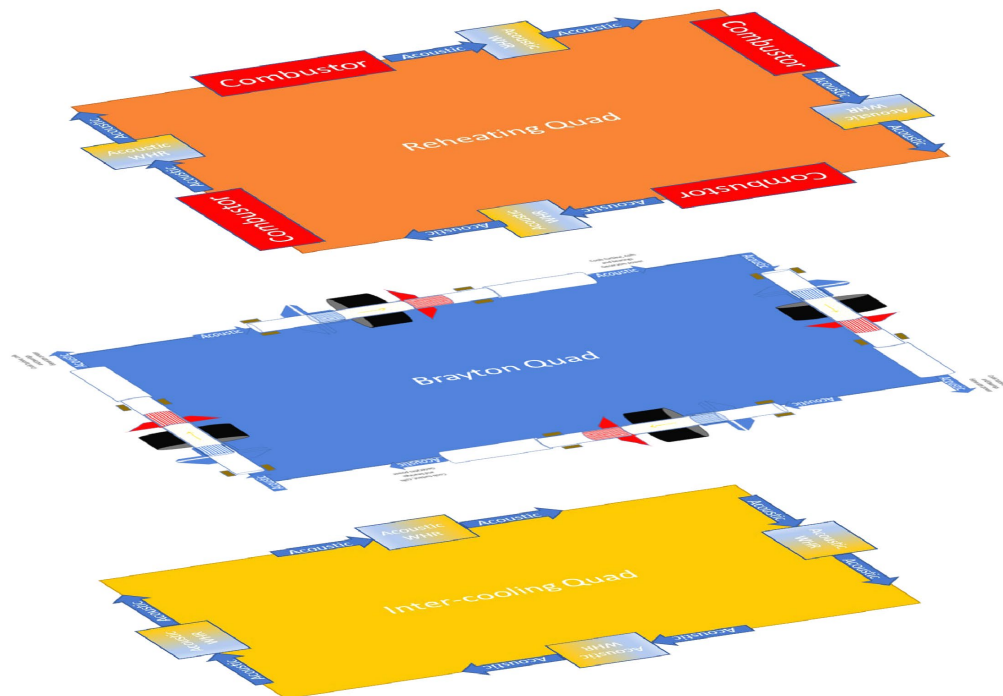


Fig. 27. Closed Strayton Quad Generator

B. Cycle Description and Performance

A full thermodynamic analysis of the Closed Strayton Quad Generator is described next. The analysis of the combustion system and the acoustic Stirling system is straight-forward and will not be shown here. It should be noted that the performance of the acoustic Stirling quad loop system can be calculated with the curves shown in Fig. 23. The combustion system performance is normally limited to about 93% effectiveness when operating at Standard Temperature and Pressure (STP), but when using a cryogenic fuel and/or at high altitude, additional recuperation effectiveness is possible as shown in Fig. 11.

1. Single Closed Strayton Unit Analysis

The first analysis is calculating the non-dimensional specific work, non-dimensional specific heat addition, and cycle efficiency of a single closed gas-turbine power cycle like the analysis shown in Fig. 18:

Specific work:

$$\dot{W}' = \frac{\dot{W}}{\dot{m}_c \bar{c}_p T_{01}} = \left(\frac{\dot{m}_e}{\dot{m}_c} \frac{\bar{c}_{pe}}{\bar{c}_{pc}} \right) E_1 T' - C \quad (1)$$

Specific heat addition:

$$\dot{Q}' = \left(\frac{\dot{Q}}{\dot{m}_c \bar{c}_p T_{01}} \right) = \left(\frac{\dot{m}_b \bar{c}_{pb}}{\dot{m}_c \bar{c}_{pc}} \right) \{ T' [1 - \varepsilon_x (1 - E_1)] - (1 + C)(1 - \varepsilon_x) \} \quad (2)$$

Cycle thermal efficiency:

$$\eta_{th} = \frac{[(\dot{m}_e/\dot{m}_c)(\bar{c}_{pe}/\bar{c}_{pc})]E_1 T' - C}{[(\dot{m}_b/\dot{m}_c)(\bar{c}_{pb}/\bar{c}_{pc})][T'^{(1-\varepsilon_x(1-E_1))} - (1+C)(1-\varepsilon_x)]} \quad (3)$$

$$E_1 = (T_{04} - T_{05})/T_{04} = 1 - \{ [(1 - \sum(\Delta p_0/p_0))r]^{(-R/\bar{c}_{pe})\eta_{pe}} \} \quad (4)$$

$$r = (p_{02}/p_{01}) \quad (5)$$

$$T' = T_{04}/T_{01} \quad (6)$$

$$C = (T_{02} - T_{01})/T_{01} = [r^{(R/\bar{c}_{pc})/\eta_{pc}} - 1] \quad (7)$$

$$\varepsilon_x = (T_{03} - T_{02})/(T_{05} - T_{02}) \quad (8)$$

2. Closed Strayton Quad Analysis

The analysis above is repeated and extended to the full four unit Closed Strayton Quad Generator.

Specific work:

$$\dot{W}' = \frac{\dot{W}}{\dot{m}_c \bar{c}_p T_{01}} = \left(\frac{\dot{m}_e}{\dot{m}_c} \frac{\bar{c}_{pe}}{\bar{c}_{pc}} \right) 4E_4 T' - 4C + 6C^2(\varepsilon_i - 1) - 4C^3(\varepsilon_i - 1)^2 + C^4(\varepsilon_i - 1)^3 \quad (9)$$

Specific heat addition:

$$\dot{Q}' = \left(\frac{\dot{Q}}{\dot{m}_c \bar{c}_p T_{01}} \right) = \left(\frac{\dot{m}_b \bar{c}_{pb}}{\dot{m}_c \bar{c}_{pc}} \right) \{ -(1 + C)(-1 + C(\varepsilon_i - 1))^3 (\varepsilon_x - 1) + T' - \varepsilon_x T' + E_4(\varepsilon_x + 3)T' \} \quad (10)$$

Strayton Quad Cycle thermal efficiency:

$$\eta_{th} = \frac{[(\dot{m}_e/\dot{m}_c)(\bar{c}_{pe}/\bar{c}_{pc})]4E_4 T' - 4C + 6C^2(\varepsilon_i - 1) - 4C^3(\varepsilon_i - 1)^2 + C^4(\varepsilon_i - 1)^3}{[(\dot{m}_b/\dot{m}_c)(\bar{c}_{pb}/\bar{c}_{pc})]\{ -(1+C)(-1+C(\varepsilon_i - 1))^3 (\varepsilon_x - 1) + T' - \varepsilon_x T' + E_4(\varepsilon_x + 3)T' \}} \quad (11)$$

$$E_4 = (T_{04d} - T_{05d})/T_{04d} = 1 - \left\{ \left[\left(1 - \left(\frac{1}{4} \right) \sum(\Delta p_0/p_0) \right) r \right]^{(-R/\bar{c}_{pe})\eta_{pe}} \right\} \quad (12)$$

$$r = (p_{02a}/p_{01a}) = (p_{02b}/p_{01b}) = (p_{02c}/p_{01c}) = (p_{02d}/p_{01d}) \quad (13)$$

$$T' = T_{04a}/T_{01a} = T_{04b}/T_{01a} = T_{04c}/T_{01a} = T_{04d}/T_{01a} \quad (14)$$

$$C = \frac{(T_{02a} - T_{01a})}{T_{01a}} = \frac{(T_{02b} - T_{01b})}{T_{01b}} = \frac{(T_{02c} - T_{01c})}{T_{01c}} = \frac{(T_{02d} - T_{01d})}{T_{01d}} = [r^{(R/\bar{c}_{pc})/\eta_{pc}} - 1] \quad (15)$$

$$\varepsilon_x = (T_{03} - T_{02d})/(T_{05d} - T_{02d}) \quad (16)$$

$$\varepsilon_i = \frac{(T_{02a} - T_{01b})}{(T_{02a} - T_{01a})} = \frac{(T_{02b} - T_{01c})}{(T_{02b} - T_{01b})} = \frac{(T_{02c} - T_{01d})}{(T_{02c} - T_{01c})} \quad (17)$$

The results are shown in Fig. 28. Note that normally the temperature ratio, Tr, is limited to about 3 in closed Brayton cycles because of the difficulty of cooling the turbine as highlighted in Fig. 17. The benefit of operating the

closed Brayton cycle at similar temperature ratios as commercial turbofans is the efficiency and specific work are now comparable when using in a single-state configuration as shown in Fig. 28(a). However, when the Closed Brayton is arranged in a quad configuration (which enables the acoustic Stirling cooling), the results shown in Fig. 28(b), indicate a three to four-fold improvement in specific work (mass) and an efficiency improvement from 58% to nearly 70%.

This analysis over-estimates performance because it does not include various parasitic losses such as bearings, windage, seals, generator, and combustion. But it under-estimates performance because the three acoustic Stirling quad loops are not included in the overall performance of the system. A full design will optimize the combustor, Brayton, and acoustic Stirling but is beyond the scope of this report.

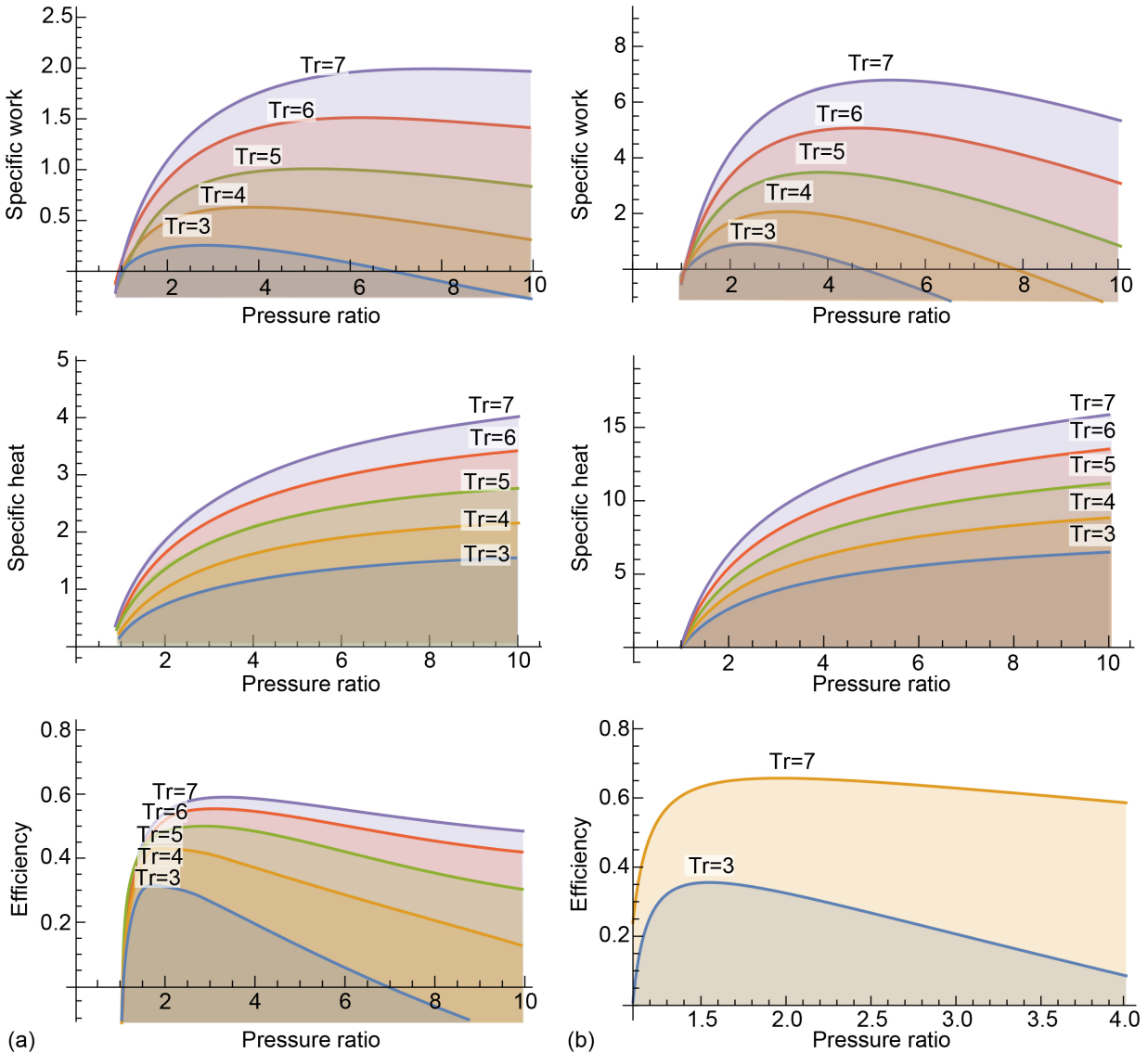


Fig. 28. Comparison of Single Closed Brayton with Quad Configuration vs. Tr and Pr Compressor Efficiency: 0.85, Turbine Efficiency: 0.90, Heat Exchanger Effectiveness: 0.9. (a) Closed Brayton. (b) Closed Brayton Quad

C. Quad Configuration Synergy

The use of a quad configuration with a combined Brayton and Stirling cycle has several unique features and advantages:

1. *The same working fluid is shared between the Brayton and acoustic Stirling cycles through a clearance seal between the rotating shaft and non-rotating hollow tube*
 - a. The inert high pressure, high molecular weight working fluid (e.g., He-Ar) makes the turbomachinery small enough to be cooled conductively and makes the bi-directional turbine over 90% efficient as shown in Fig. 14. This is another key synergy between Brayton and Stirling both benefiting from the same working fluid but for different reasons.
 - b. The sealed pressurized inert working fluid also enables the use of gas bearings instead of oil bearings. This results in a no-maintenance system. But it also enables a zero-greenhouse gas emission because no oil particulates are released into the atmosphere from the oil bearings (forms contrails). It also enables very high-speed rotation that is not normally possible with oil bearings, and this significantly reduces the size of the turbomachinery and generator.
 - c. The fuel cell can be replaced with a steam mixer to achieve longer life in the combustion system. The steams come from the exhaust itself when burning hydrogen.
2. *The quad configuration is a unique performance enhancer for both Brayton and Stirling:*
 - a. Brayton impact
 - i. Compressor efficiency increases quickly up to 4 stages (benefits decline at >4 stages)
 - ii. Turbine efficiency increases quickly up to 4 stages (benefits decline at >4 stages)
 - iii. Momentum is naturally cancelled from two pairs rotating in opposite directions
 - b. Acoustic Stirling impact
 - i. Allows the Stirling regenerators to be separated by $\frac{1}{4}$ of the wavelength which means no flywheel or resonator is required. Like a piston car engine, there is always power being inserted into the cycle. A Stirling cycle naturally wants a 90° phase difference between pressure wave and displacement.
 - ii. The four 90° results in a full 360° cycle around which allows the cycle to repeat exactly. We don't need to generate an incoming acoustic wave since it is already perfectly timed from the previous wave that traveled around. This makes the system much smaller than typical thermoacoustic engines.
 - iii. The looped configuration allows the amplification of the system to continue to grow until it reaches the maximum the heat exchangers can support. Without the loop, the acoustic wave can only be amplified by a factor 3 and wouldn't provide nearly as much turbine cooling.

VIII. High-Speed Switched Reluctance Generator

By virtue of their simple and robust rotor construction without embedded permanent magnets or electrical windings, switched reluctance (SR) machines, shown in Fig 28, are mechanically capable of very high-speed and higher temperature operation which makes them a perfect fit for Closed Strayton Quad Generator which intentionally transports heat from the turbine through the shaft to the compressor exit. Furthermore, their specific power output can exceed permanent magnet generators at very high speeds. The higher shaft speed reduces the volume, V , of both the turbomachinery and generator:

$$V \propto \frac{P_{out}}{A_1 B_g n}$$

for the same stator line current density A_1 and airgap magnetic flux density B_g where P_{out} is the output power [Gieras].

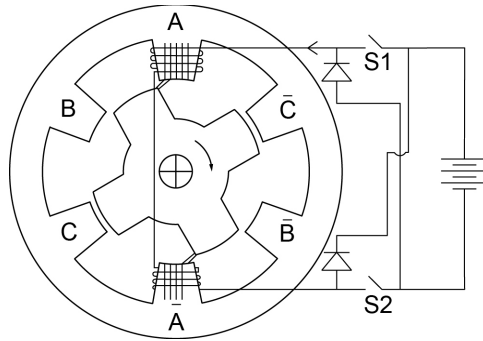


Fig. 29. High-Speed, High-Temperature, High-Specific Power, High Efficiency, Fault-Tolerant Switched Reluctance Generator (SRG)

There is therefore an attraction in using SR machines for high-speed generator applications where weight and space are important considerations.

PM generators are an alternative as well but suffer from several potential drawbacks:

1. Present cost of permanent magnet materials and rare earth material availability.
2. Because it is not possible to vary the excitation of a PM generator, a potential disadvantage is poor voltage regulation.
3. In the event of a winding fault, the generator can only be deenergized by mechanically decoupling the generator from the engine or prime mover.
4. High temperature (above 300 °C) environment in particular applications may prohibit the use of PM generators unless sufficient cooling can be supplied. This is mainly due to a limitation in the maximum application temperatures of rare earth magnetic materials.
5. PM generators inherently produce variable voltage variable frequency (or wild voltages and frequencies).
6. There will be lower efficiencies and higher losses at light loads and specially at no-load. In general, PM machines have high impedances and must be operated near their maximum output.
7. The placement of permanent magnets on the surface of the rotor causes problems in spinning the rotor at very high speeds (above 15,000 rpm). A more adequate mechanical strength may be provided for the rotor by using a can, which may consist of magnetic or non-magnetic material, to contain the rotor. This, however, is likely to reduce the overall output of the machine.
8. Magnet corrosion and possible demagnetization are potential hazards do not present with other technologies.
9. The machining required for all the available magnets is hard, and consequently expensive, as these materials are known to be brittle. The NdFeB is, however, an exception.

For these reasons, a three-phase Switched Reluctance Generator is installed on the rotating Brayton shaft since we have both high speed and high temperatures in a Closed Strayton Quad Generator. It should be noted that operating at higher temperatures in space reduces radiator mass as well. Also, the SRG will still operate even during a fault of one of its phases [82-89].

IX. Benefits Summary

In summary, the Closed Strayton Quad Generator invention carries the following benefits:

A. Open and Closed Strayton Benefits

1. Higher turbine inlet temperature via conductive cooling of the turbine from the embed acoustic Stirling cycle increases Brayton efficiency
2. Higher thermal recuperation with thermal transfer from the turbine to the compressor exhaust via acoustic Stirling cycle transport increases Brayton efficiency
3. Higher system efficiency by providing thermoacoustic topping and bottoming cycles
4. Reduces the size of the heat exchangers with acoustic quad loops heat transfer
5. Thermoacoustic cooling can be used to refrigerate the generator, bearings, and electronics

B. Unique Closed Strayton Benefits

1. Separation of the heat source from the turbine inlet fluid
 - a. Enables use of nuclear, solar, or combustion heat source with same technology
 - b. Protects turbine blades from combustion products, reactivity, and creep
2. Enables use of higher-pressure working fluid for higher specific power at any altitude
3. Enables use of pressurized gas-bearings that support very high-speed no-maintenance shafts that reduce the overall turbomachinery and generator mass
4. Enables higher temperature turbine blades that normally is not possible in a closed system due to limited blade cooling options and refractory coating limitations

The performance gains to be realized are significant because of the following unique features:

1. The ability to cool the turbine blade conductively with an embedded thermodynamic cycle enables operating the Brayton cycle at higher compression ratio and hence efficiency.
2. The waste heat from cooling the turbine blade and rejected heat exhaust is used to power the Stirling engine that is embedded in the shaft (acting as a bottoming cycle).
3. The rejected heat from the Stirling engine is used to heat the compressed Brayton working fluid (acting as a recuperator and topping cycle for the Brayton). In this way, the Brayton and Stirling mutually serve as Topping and Bottoming cycles at the same time for maximum system efficiency!
4. By closing the entire system into a hermetically sealed unit, the Brayton and Stirling working fluid can be pressurized to increase the specific power which reduces the turbine diameter to less than 4 inches at MW-scale, making it a highly effective conductive heat transfer component for both turbine cooling and compressor outlet heating.
5. Normally a closed Brayton cycle requires a very large recuperator that dominates the mass of the entire system, but the Stirling cycle naturally provides recuperation when it acoustically transfers the waste heat from the turbine end to the compressor end.
6. No gearbox is required because the rotational speed can be perfectly matched with the required generator speeds (due to sealed working fluid and pressure tuning).
7. The sealed system is perfectly quiet.
8. Relaxed tolerances reduce manufacturing costs because the dual topping/bottoming cycle synergy reduces the need for separate high efficiency components (one cycle's loss is the other cycle's gain).
9. The hermetically sealed Brayton and Stirling cycles enable the use of inert working fluids to eliminate corrosion (typically noble gases). The noble gas working fluids enables higher operating temperatures because they don't corrode like $s\text{CO}_2$ at $>923\text{K}$, are more compatible with higher temperature refractory turbine blades (no oxygen), and when combined with the embedded conductive cooling of the Stirling cycle potentially enables $>1500\text{K}$ inlet temperatures for even higher efficiency.
10. The $s\text{CO}_2$ heat rejection constraint (critical point temperature of $\sim 310\text{K}$) requires large heat exchangers, but noble gases can reject at higher temperatures useful for aero and space heat exchanger mass rejection.
11. Strayton Quad Generator has a compact size and natural momentum cancelling.
12. It is heat source agnostic which enables zero-emission or sustainable fuels to be used for aircraft and nuclear sources for terrestrial and space applications.
13. The inert working fluid does not require the very high pressures that $s\text{CO}_2$ requires (2 MPa vs. 25 MPa) which reduces system mass.
14. The entire system is hermetically sealed with no moving external seals.

C. Fault Tolerance

The Strayton Quad Generator has the following inherent redundancy and fault-tolerant advantages:

- Each generator voltage, and power output can be independently controlled simplifying power management and distribution
- Over-speed risk from no load is reduced from independent stator phases and mass flow limits imposed by the quad configuration
- Material creep and corrosion is mitigated by active cooling of the turbomachinery
- Each quad loop still functions under multiple fault conditions
- Each Brayton can be locked independently, and the working fluid still can circulate

- Each Stirling generator can fail but the acoustic loop will continue to function
- Quad configuration provides four redundant Brayton power generators and up to three redundant Stirling power generators
- Compressor stall and surge is controlled electrically
- Typical temperature limits no longer apply

X. Conclusion

A true zero emission electric propulsion system for transport class aircraft was presented that leverages a recently invented Closed Brayton Quad Generator technology to potentially eliminate all greenhouse gas emissions in a clean power generation system that is lighter and lasts longer than fuel cells at the megawatt power level required for transport aircraft propulsion. The hermetically sealed working fluid of these units enables no-maintenance gas bearings, non-corrosive working fluids, compact, highly efficient, quiet, environmentally benign, and low-cost power generation.

The technology enables the separate optimization of power generation, electric propulsion, and combustion resulting in new true zero GHG emission powertrain options. This allows for novel electric fan propulsors such as contra-rotating and advanced noise cancellation configurations. The high efficiency and specific power combined with advanced propulsors can potentially achieve higher overall efficiency than today's turbofans. But even if it can't fully match turbofans, it introduces a new way to manage emissions and noise that the public may find outweighs some losses in mass and efficiency. It should be noted that using hydrogen fuel that is three times lighter than jet fuel may compensate for the extra heat exchanger mass that this closed cycle system incurs. The proposed technology also supports the gradual transition of fuel from kerosene to SAF to hydrogen by acting as a secondary power source that supplements hybrid electric propulsors but does so with onboard clean energy generation. This allows for the economic transition of today's infrastructure while still achieving significant emission benefits in the nearer term.

The next steps for this technology are to finish building out the technology to include the optimized combustor system for reheating and the three acoustic Stirling loops. However, it should be noted that the three basic technologies outlined in this report including: Closed cycle Brayton, Closed cycle acoustic Stirling loop, and NO_x managed combustion have been demonstrated previously. The new part is integrating them together in this novel way.

Appendix—Open Strayton Generator Configurations

The previously shown Closed Strayton configurations can also be converted to Open Cycle in which external air is delivered through both the combustor and turbomachinery as is typical with commercial turbofans. Shown in Fig. 30 is a basic open cycle for a single Strayton.

The next series of schematics show the quad configuration in a linear cascade format for easier documentation. Fig. 31 shows a very simple open cycle, reheated stage, with no recuperation.

Fig. 32 adds in recuperation, again note only one recuperator is needed for four Strayton cycles.

Fig. 33 adds in inter-cooling between each compressor stage using an acoustic Stirling quad heat exchanger.

Fig. 34 adds in prewarming of the fuel between each combustion stage using an acoustic Stirling quad heat exchanger.

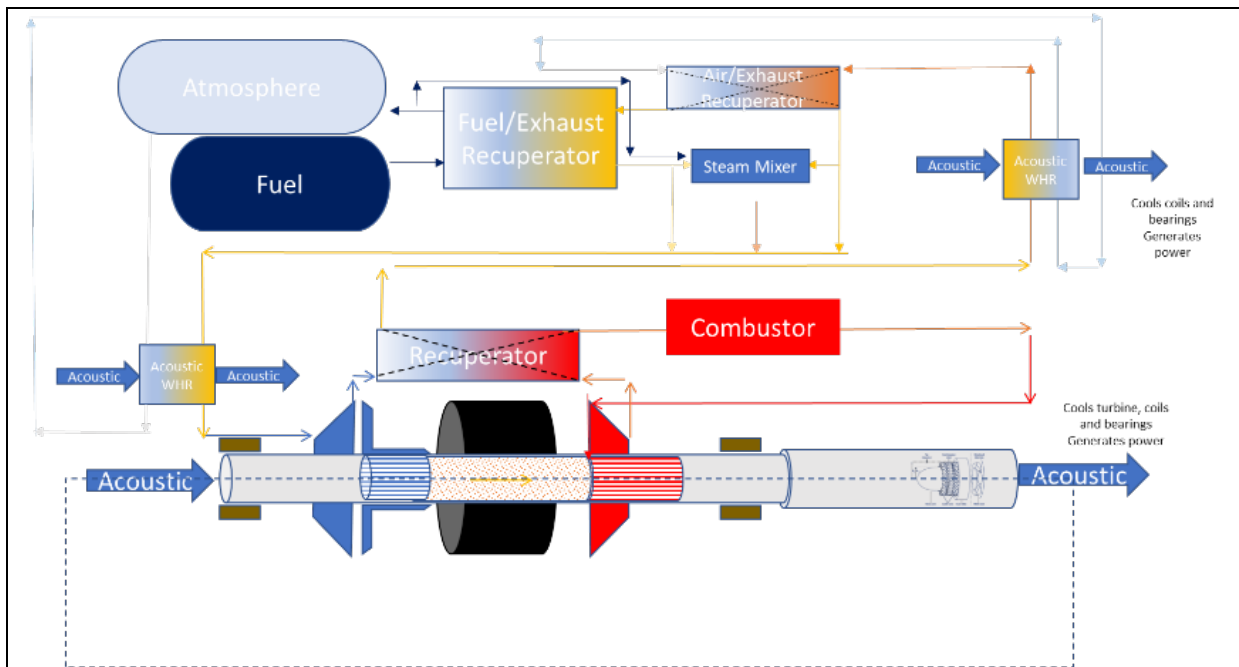


Fig. 30. Open cycle with recuperation

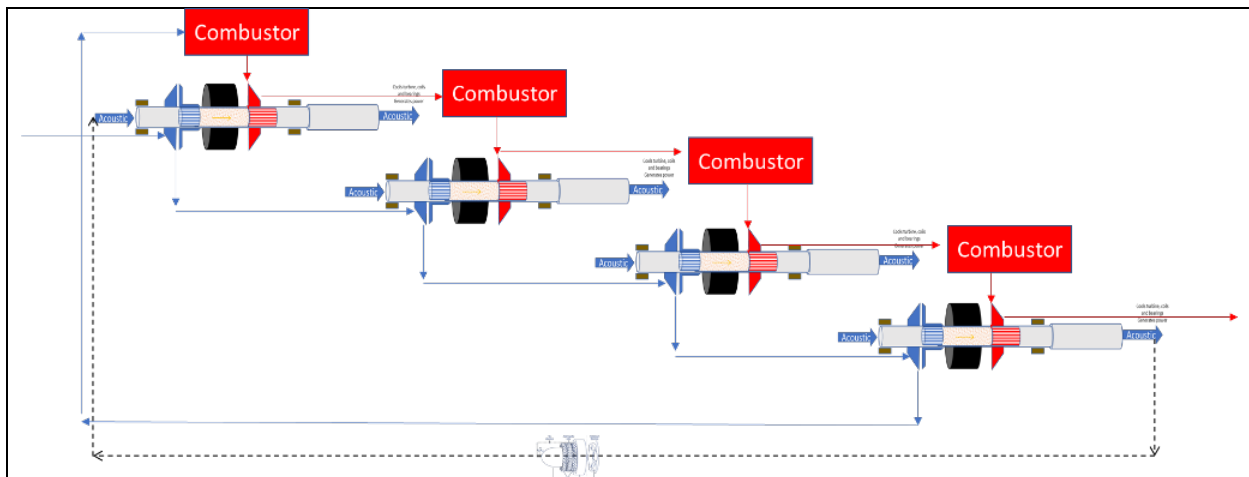


Fig. 31. Simple open cycle no recuperation

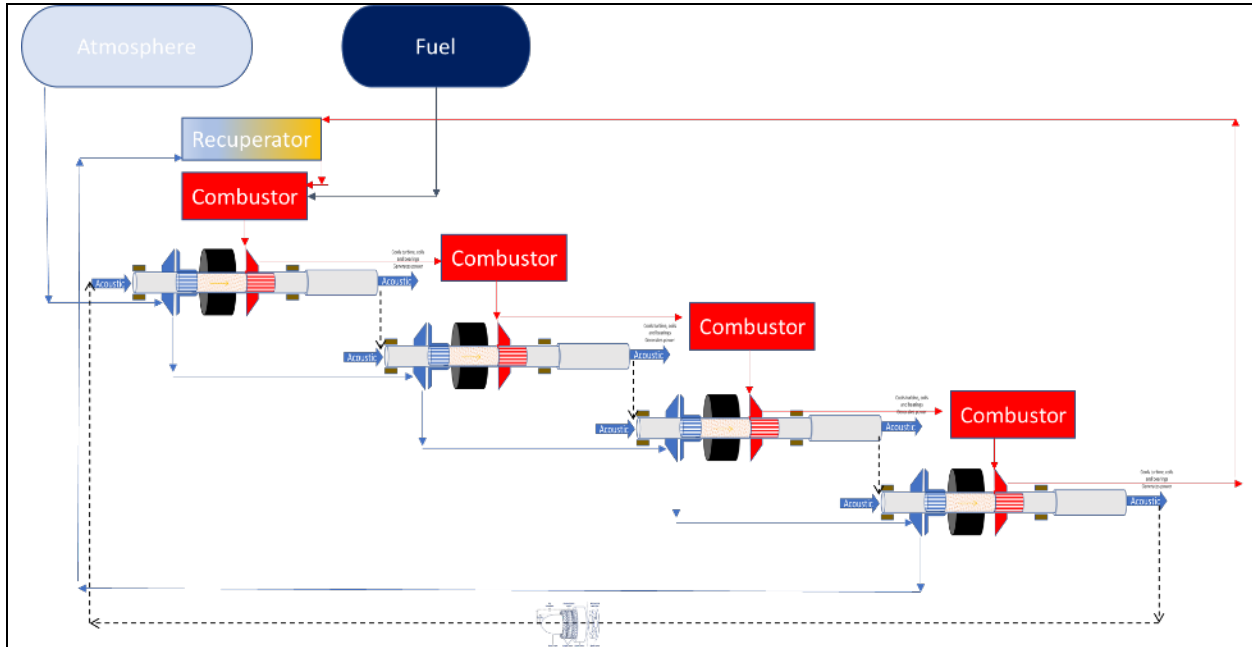


Fig. 32. Simple open cycle with recuperation

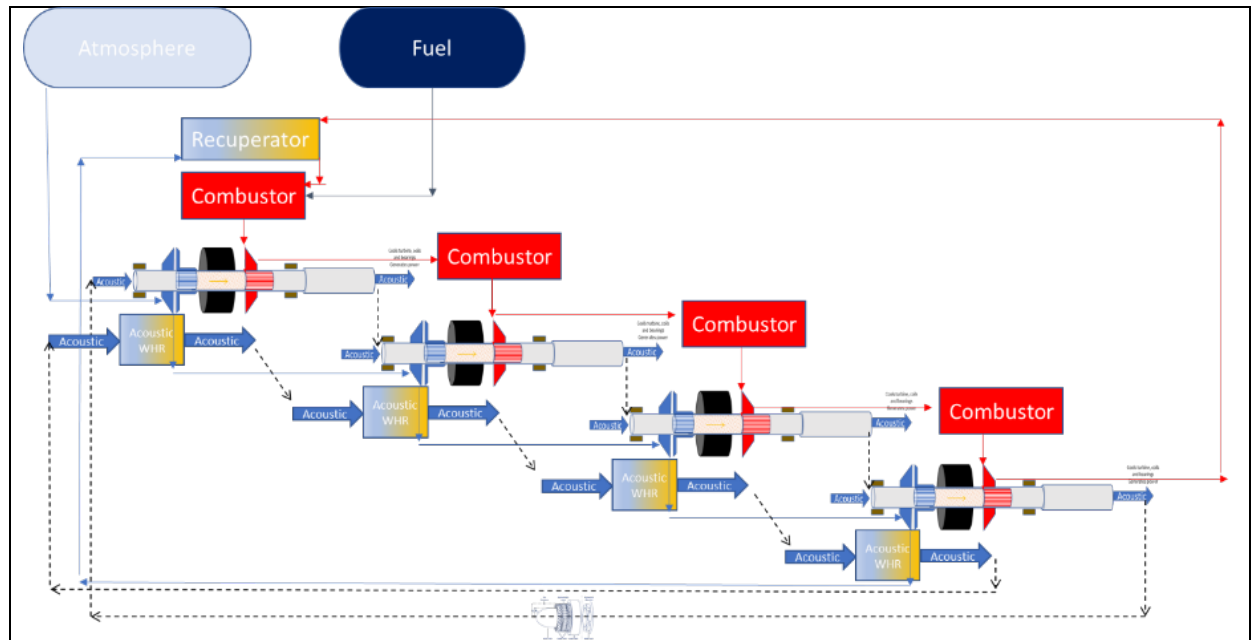


Fig. 33. Open Cycle, Acoustic Intercool

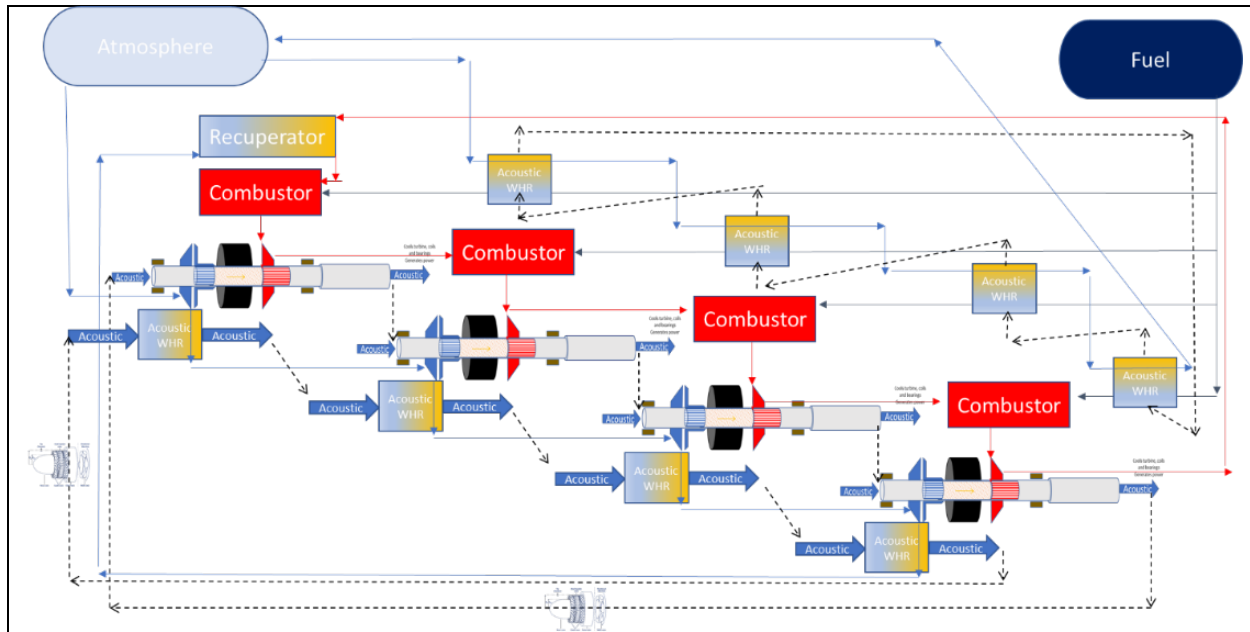


Fig. 34. Open Cycle, Recuperated, Acoustic intercool/reheat

Acknowledgments

The author thanks the Advanced Aircraft Transportation Technology project and Space Nuclear Propulsion project for their support of this work. This technology is patent pending.

References

Climate/Emissions

1. Bloomberg News, "Biden Urges Net-Zero Aviation by 2050 in Leap Beyond Cars," November 9, 2021, <https://www.bloomberg.com/news/articles/2021-11-09/>, accessed on: Aug. 14, 2022.
2. B. Graver, D. Rutherford, and S. Zheng, "CO2 Emissions from Commercial Aviation," Oct. 2020.
3. D. S. Lee and etc., "The contribution of global aviation to anthropogenic climate forcing for 2000 to 2018", Atmospheric Environment vol. 244, 1 January 2021.
4. Advancing NASA's Climate Strategy, 2023
5. IPCC Special Report, Aviation and the Global Atmosphere, 1999
6. DOE National Clean Hydrogen Strategy and Roadmap Draft - September 2022
7. Opportunities for hydrogen in commercial aviation, Boeing, CSIRO
8. Carbon Neutral Commercial Aviation NASA Glenn Coordination Meeting ARPA E Aviation Team April 8, 2021
9. Lee, D.S. et al, The contribution of global aviation to anthropogenic climate forcing for 2000 2018, Atmospheric Environment 244 (2021)
10. EIA Annual Energy Outlook 2020
11. ARPA-E Aviation Intro 2022

Hydrogen/Aircraft

12. Khan, M.A.H.; Brierley, J.; Tait, K.N.; Bullock, S.; Shallcross, D.E.; Lowenberg, M.H., "The Emissions of Water Vapour and NOx from Modelled Hydrogen-Fuelled Aircraft and the Impact of NOx Reduction on Climate Compared with Kerosene-Fuelled Aircraft," Atmosphere 2022, 13, 1660.
13. Eytan J. Adler and Joaquim R. R. A. Martins. "Hydrogen-Powered Aircraft: Fundamental Concepts, Key Technologies, and Environmental Impacts." Progress in Aerospace Sciences (2023).
14. Khan, M.A.H.; Brierley, J.; Tait, K.N.; Bullock, S.; Shallcross, D.E.; Lowenberg, M.H., "The Emissions of Water Vapour and NOx from Modelled Hydrogen-Fuelled Aircraft and the Impact of NOx Reduction on Climate Compared with Kerosene-Fuelled Aircraft. Atmosphere 2022, 13, 1660.
15. Choi, Y.; Lee, J., "Estimation of Liquid Hydrogen Fuels in Aviation," Aerospace 2022, 9, 564
16. A. C. Lewis, "Optimising air quality co-benefits in a hydrogen economy: a case for hydrogen-specific standards for NOx emissions," Environmental Science: Atmospheres.

17. Christopher A. Snyder, Jeffrey J. Berton, Gerald V. Brown, James L. Dolce, Narayan V. Dravid, Dennis J. Eichenberg, Joshua E. Freeh, Christopher A. Gallo, Scott M. Jones, Krishna P. Kundu, Cecil J. Marek, Marc G. Millis, Pappu L. Murthy, Timothy M. Roach, Timothy D. Smith, George L. Stefko, Roy M. Sullivan, and Robert T. Tornabene, Karl A. Geiselhart, Albert F. Kascak, "Propulsion Investigation for Zero and Near-Zero Emissions Aircraft," NASA/TM—2009-215487
18. G. Onorato, P. Proesmans, M.F.M. Hoogreef, "Assessment of hydrogen transport aircraft Effects of fuel tank integration," CEAS Aeronautical Journal, June 2022
19. Jonas Mangold, Felix Brenner, Nicolas Moebs and Andreas Strohmayr, "Aircraft Design Implications of Alternative Fuels for Future Hybrid-Electric Regional Aircraft Configurations," 9th European Conference For Aeronautics and Space Sciences, 2022
20. Alastair C. Lewis, Optimising air quality co-benefits in a hydrogen economy: a case for hydrogen-specific standards for NOx emissions, *Environ. Sci.: Atmos.*, 2021, 1,201
21. Hydrogen Infrastructure and Operations Airports, Airlines and Airspace, FZO-CST-POS-0035 Published March 2022, Aerospace Technology Institute – FlyZero - Hydrogen Infrastructure and Operations, FZO-CST-POS-0035
22. 2001 Assessment of Using Liquid Hydrogen as a Fuel in Conventional Gas turbine Engines, Propulsion Systems Analysis Office, NASA Glenn, September 2001 Assessment
23. Jayant Mukhopadhyaya, PhD and Brandon Graver, PhD, Performance Analysis of Regional Electric Aircraft, International Council on Clean Transportation, July 2022
24. Wolfgang Stautner, Phillip J. Ansell, and Kiruba S. Haran, CHEETA: An All-Electric Aircraft Takes Cryogenics and Superconductivity on Board Combatting climate change. *IEEE Electrification Magazine*, June 2022
25. Ausilio Bauen, Niccolò Bitossi, Lizzie German, Anisha Harris, Khangzhen Leow, Sustainable Aviation Fuels Status, challenges and prospects of drop-in liquid fuels, hydrogen and electrification in aviation, *Johnson Matthey Technol. Rev.*, 2020, 64, (3), 263–278
26. Jack Brouwer, 1.4 Hybrid Gas Turbine Fuel Cell Systems, National Fuel Cell Research Center University of California, 2005
27. Elias G. Waddington, Jason M. Merret, and Phillip J. Ansell, Impact of LH2 Fuel Cell-Electric Propulsion on Aircraft Configuration and Integration, *AIAA Aviation 2021 Forum*, August 2-6, 2021
28. Pedro D. Bravo-Mosquera, Fernando M. Catalano, David W. Zingg, Unconventional aircraft for civil aviation: A review of concepts and design, *Progress in Aerospace Sciences* 131 (2022) 100813
29. Christopher A. Snyder, H2/DeCarbonization studies: history and ongoing, November 10, 2021
30. Jane O'Malley, Nikita Pavlenko, Stephanie Searle, Estimating sustainable aviation fuel feedstock availability to meet growing European Union demand, Working Paper 2021-13, International Council On Clean Transportation, March 2021
31. Elias G. Waddington, Jason M. Merret, and Phillip J. Ansell, Impact of Liquid-Hydrogen Fuel-Cell Electric Propulsion on Aircraft Configuration and Integration, *AIAA Journal of Aircraft*, March 2023
32. Eissele, J.; Lafer, S.; Mejía Burbano, C.; Schließus, J.; Wiedmann, T.; Mangold, J.; Strohmayr, A. Hydrogen-Powered Aviation—Design of a Hybrid-Electric Regional Aircraft for Entry into Service in 2040. *Aerospace* 2023, 10, 277
33. Alastair Lewis, Optimising air quality co-benefits in a hydrogen economy: a case for hydrogen-specific standards for NOx emissions, *Environ. Sci.: Atmos.*, 2021, 1, 201

Fuel Cell

34. Stefan Kazula, Stefanie de Graaf, Lars Enghardt, "Preliminary Safety Assessment of PEM Fuel Cell Systems for Electrified Propulsion Systems in Commercial Aviation," Proceedings of the 32nd European Safety and Reliability Conference (ESREL 2022)
35. A. Datta, "PEM Fuel Cell Model for Conceptual Design of Hydrogen eVTOL Aircraft," NASA/CR—20210000284, Jan. 2021.
36. Fafu Guo, Chengjie Li, He Liu, Kunlin Cheng, Jiang Qin, "Matching and performance analysis of a solid oxide fuel cell turbine-less hybrid electric propulsion system on aircraft", *Energy* 263 (2023)
37. Ryan Russell Sinnamon, "Analysis of a Fuel Cell Combustor in a Solid Oxide Fuel Cell Hybrid Gas Turbine Power System For Aerospace Application," Wright State University, 2012
38. Fuel Cells, H2fly. <https://www.h2fly.de/>

Acoustics

39. Swift, Gregory W.: Thermoacoustics.
40. Timmer MAG, de Blok K, van der Meer TH, "Review on the conversion of thermoacoustic power into electricity," *J Acoust Soc Am*. 2018 Feb;143(2):841
41. Michael Timmer, bidirectional impulse turbines for thermoacoustic devices, Thesis, Universiteit Twente, 2020
42. Jingyuan Xua, Ercang Luob, Simone Hochgreba, Study on a Heat-Driven Thermoacoustic Refrigerator for Low-Grade Heat Recovery, 2020
43. Kees de Blok, Multi-Stage Traveling Wave Thermoacoustics In Practice, ICSV19, Vilnius, Lithuania, July, 2012, 19th International Congress on Sound and Vibration, Vilnius, Lithuania, July 8-12, 2012

44. D. L. Gardner and G. W. Swift, A cascade thermoacoustic engine, *The Journal of the Acoustical Society of America* 114, 1905 (2003);
45. Isares Dhuchakallay and Patcharin Saechan, Design and experimental evaluation of a travelling-wave thermoacoustic refrigerator driven by a cascade thermoacoustic engine, *Int J Energy Res.* 2018;42:3059–3067
46. Sudeep Sastry, A Thermoacoustic Engine Refrigerator System For Space Exploration Mission, thesis, Case Western Reserve University, May 2011
47. Dhananjay G. Thombare and Suhas V. Karmare, Theoretical and experimental investigation of Alfa type bio mass Stirling engine with effect of regenerator effectiveness, heat transfer, and properties of working fluid, *J. Renewable Sustainable Energy* 4, 043126 (2012)

Bi-Directional Acoustic Turbines

48. Kees de Blok, Pawel Owczarek, Maurice-Xavier Francois, “Bi-directional turbines for converting acoustic wave power into electricity,” <http://www.aster-thermoacoustics.com/wp-content/uploads/2015/01/Bi-directional-turbines-Riga.pdf>, 2015
49. A. Thakker, J. Jarvis, and A. Sahed, Quasi-Steady Analytical Model Benchmark of an Impulse Turbine for Wave Energy Extraction, *International Journal of Rotating Machinery* Vol. 2008, Article ID 536079, 12 pages
50. Bruno Pereiras, Francisco Castro, Abdelatif el Marjani, Miguel A. Rodríguez, An improved radial impulse turbine for OWC, *Renewable Energy* 36 (2011) 1477e1484
51. Toshiaki Setoguchi a, Manabu Takao, Current status of self rectifying air turbines for wave energy conversion, *Energy Conversion and Management* 47 (2006) 2382–2396
52. Mina Saad, Manuel García Díaz, Bruno Pereiras, Jose Gonzalez, Optimized geometry design of a radial impulse turbine for OWC wave energy converters, *Applied Ocean Research* 111 (2021) 102650

Brayton Turbogeneration

53. Albert J. Juhasz, Gas Turbine Energy Conversion Systems for Lunar/Mars “HTGR” Nuclear Power Plants and Liquid Fluoride Thorium Reactor “LFTR” Technology for Ground Based Applications Part 1: Gas Turbine Thermodynamics, March 17, 2022
54. Nuclear Electric Propulsion Brayton Power Conversion Working Fluid Considerations. Rodger Dyson et al., *Nuclear and Emerging Technologies for Space (NETS-2022)*, 2022. <https://ntrs.nasa.gov/citations/20220002293>
55. Robert L. Fuller, Closed Brayton Cycle Power Conversion Unit for Fission Surface Power Phase I Final Report, NASA/CR—2010-215673
56. Steven A. Wright, Preliminary Results of a Dynamic System Model for a Closed-Loop Brayton Cycle Coupled to a Nuclear Reactor, 1st International Energy Conversion Engineering Conference 17 - 21 August 2003, Portsmouth, Virginia
57. John Foti, David Halsey, Tim Bauch, “Applicability of Aircraft Brayton Power Technologies To Future Space Power Conversion Systems,” 2002 37th Intersociety Energy Conversion Engineering Conference (IECEC)
58. Rodger Dyson, D. V. Rao, Matthew Duchek, Christopher Harnack, Robert Scheidegger, Lee Mason, Al Juhasz, Luis Rodriguez, Ronald Leibach, Steven Geng, Daniel Goodell, “Nuclear Electric Propulsion Brayton Power Conversion Working Fluid Considerations,” *Nuclear Emerging Technologies for Space 2022*, Cleveland, OH, May 2022
59. Mohamed S. El-Genk, Jean-Michel Tournier, Effects of working fluid and shaft rotation speed on the performance of HTR plants and the size of CBC turbo-machine
60. ULTIMATE—Ultrahigh Temperature Impervious Materials Advancing Turbine Efficiency, arpa-e, 2022
61. Nageswara Rao Muktinatalapati, “Materials for Gas Turbines – An Overview”, *Advances in Gas Turbine Technology*, INTECH, 2011
62. Dixon, S.L.: *Fluid Mechanics and Thermodynamics of Turbomachinery*.
63. Albert J. Juhasz, Analysis and Numerical Optimization of Gas Turbine Space Power Systems With Nuclear Fission Reactor Heat Sources, Thesis, Cleveland State University May, 2005
64. John Foti, Dave Halsey, Tim Bauch, Technology Concept for a Near-Term Closed Brayton Cycle Power Conversion Unit, AIP Conference Proceedings 608, 865 (2002)
65. Benoit Picard, Mathieu Picard, Jean-Sébastien Plante, David Rancourt, Enabling Sub-Megawatt Hybrid-Electric Propulsion through High Efficiency Recuperated Inside-out Ceramic Turbogenerator, STO-MP-AVT-323, 2018
66. Olumide Olumayegun, Study of Closed-Cycle Gas Turbine For Application To Small Modular Reactors (SMRs) And Coal-Fired Power Generation Through Modelling and Simulation, thesis, The University of Sheffield Faculty of Engineering Department of Chemical and Biological Engineering November 2017
67. Jussi Saari, Heat Exchanger Dimensioning, Lappeenranta University of Technology Faculty of Technology LUT Energy, 2007
68. Mohamed S. El-Genk, Jean-Michel Tournier, Noble gas binary mixtures for gas-cooled reactor power plants, *Nuclear Engineering and Design* 238 (2008) 1353–1372
69. Alan H. Epstein, Millimeter-Scale, Mems Gas Turbine Engines, *Proceedings of ASME Turbo Expo 2003. Power for Land, Sea, and Air*, June 16-19, 2003, Atlanta, Georgia, USA
70. Jurandir Primo, Shell and Tube Heat Exchangers – Basic Calculations, PDHonline Course M371 (2 PDH), 2020

71. Ji, Z.; Guo, F.; Zhu, T.; Cheng, K.; Zhang, S.; Qin, J.; Dong, P. Thermodynamic Performance Comparisons of Ideal Brayton Cycles Integrated with High Temperature Fuel Cells as Power Sources on Aircraft. *Sustainability* 2023, 15, 2805.
72. Jean-Michel P. Tournier and Mohamed S. El-Genk, Properties of Helium, Nitrogen, and He–N₂ Binary Gas Mixtures, *Journal of Thermophysics And Heat Transfer*, Feb. 2008
73. Mohamed S. El-Genk, Jean-Michel Tournier, Effects of working fluid and shaft rotation speed on the performance of HTR plants and the size of CBC turbo-machine, *Nuclear Engineering and Design* 239 (2009) 1811–1827
74. Prakash Prashanth, Raymond L. Speth, Sebastian D. Eastham, Jayant S. Sabnis and Steven R. H. Barrett, Post-combustion emissions control in aero-gas turbine engines, *Energy Environ. Sci.*, 2021, 14, 916
75. Olumide Olumayeguna, Meihong Wang, Greg Kelsall, Closed-Cycle Gas Turbine for Power Generation: 1 A State-of-the-Art Review, ALSTOM Power LTD, U.K., Fuel, September 2016
76. Steven A. Wright, Ronald J. Lipinski, Milton E. Vernon, Travis Sanchez, Closed Brayton Cycle Power Conversion Systems for Nuclear Reactors: Modeling, Operations, and Validation, Sandia Report SAND2006-2518 Unlimited Release Printed April 2006
77. Mohamed S. El-Genk and Jean-Michel P. Tournier, Small Size Turbo-Machines For HTR Plants, POWER2009-81171, Proceedings of the ASME 2009 Power Conference, July 21-23, 2009, Albuquerque, New Mexico
78. Willemja Nsen and Andreams . Kirschner, Impeller Blade Design Method for Centrifugal Compressors, *Turbomachinery Design*, 1975
79. Steven A. Wright, Milton E. Vernon, Paul S. Pickard, Concept Design for a High Temperature Helium Brayton Cycle with Interstage Heating and Cooling, Sandia Report SAND2006-4147 Unlimited Release Printed December 2013
80. Kangsoo Im, Development of a Design Method For Centrifugal Compressors, thesis, Michigan State University, 2012
81. Jean-Michel Tournier and Mohamed S. El-Genk, Alternative Working Fluids to Reduce Size of Turbomachinery for VHTR Plants, Proceedings of ICAPP '08, Anaheim, CA USA, June 8-12, 2008 Paper 8072

Switched Reluctance Generator

82. Thomas Heese Juha Pyrhonen, Design of a Switched Reluctance Generator, Lappeenranta University of Technology, Research Report EN A-33, 1996
83. Mohammed Taha Ebrahim, A Very High Speed Switched Reluctance Generator, Thesis, University Of Nottingham, January 1995
84. Arunava Mitra, Senior Member, IEEE, and Ali Emadi, Senior Member, IEEE, On the Suitability of Large Switched Reluctance Machines for Propulsion Applications, McMaster University, Hamilton, Ontario, Canada, 2012 IEEE
85. Boldea, Ion; and Nasar, Syed A.: *Electric Drives*. (3rd ed.)
86. Kiruba Haran, *Electric/Hybrid-Electric Drives for Aircraft Propulsion*, 2021
87. B. Fahimi, G. Suresh, M. Ehsani, Large Switched Reluctance Machines: A 1 MW Case Study, Department of Electrical Engineering, UTexas A&M University, 1999 IEEE
88. Samith Sirimanna, Xiaolong Zhang, Kiruba Haran, Investigation of the impact of magnet segmentation on high frequency eddy current losses in an interior permanent magnet motor, 2022 IEEE Energy Conversion Congress and Exposition (ECCE)
89. Jacek F. Gieras, Comparison of High-Power High-speed Machines: Cage Induction versus Switched Reluctance Motors, United Technologies Research Center, 1999 IEEE

Strayton

90. Chapman, J.W.; Simon, D.L.; McNichols, E.O.: An Analysis of the Strayton Engine, a Brayton and Stirling Cycle Recuperating Engine (Presentation). NASA Glenn Research Center, AIAA Propulsion and Energy Forum, Indianapolis, IN, Aug. 19-22, 2019. <https://ntrs.nasa.gov/api/citations/20190030499/downloads/20190030499.pdf>
91. Dyson, R.: Novel Thermal Energy Conversion Technologies for Advanced Electric Air Vehicles. Published 8 July 2018 Engineering 2018 AIAA/IEEE Electric Aircraft Technologies Symposium (EATS). DOI:10.2514/6.2018-4993 Corpus ID: 54444299. <https://www.semanticscholar.org/paper/Novel-Thermal-Energy-Conversion-Technologies-for-Dyson/0a1d7dc421565096284ce60f6bb4f2d3de27153a>
92. Chapman, J.W.; Simon, D.; McNichols, E.: An Analysis of the Strayton Engine, a Brayton and Stirling Cycle Recuperating Engine (Paper). Published 16 August 2019 Engineering AIAA Propulsion and Energy 2019 Forum, DOI:10.2514/6.2019-3826 Corpus ID: 202097252. <https://www.semanticscholar.org/paper/An-Analysis-of-the-Strayton-Engine%2C-a-Brayton-and-Chapman-Simon/60c55927c22bd6b8ad05269e578e8f52f5c2b72c>
93. Prakash Prashanth, Raymond L. Speth, Sebastian D. Eastham, Jayant S. Sabnis, and Steven R. H. Barrett, “Post-combustion emissions control in aero-gas turbine engines,” *Energy Environ. Sci.*, 2021,14, 916
94. R. Dyson, provisional patent filed May 6, 2022
95. D.G. Wilson, “The Design of High-Efficiency Turbomachinery and Gas Turbines,” MIT Press, 1984

Contra-Rotating Propulsor

96. Imon Chakraborty, Aashutosh Aman Mishra, Dennis van Dommelen, and Willem A. J. Anemaat, Design and Sizing of an Electrified Lift-Plus-Cruise Ducted Fan Aircraft, *AIAA Journal of Aircraft*, November 2022

97. J. S. Vanderover and K. D. Visser, "Analysis of a Contra-Rotating Propeller Driven Transport Aircraft," AIAA Student Paper Competition, 2006, Syracuse, NY, USA.
98. B. T. Blumenthal, "Computational Investigation of a Boundary-Layer Ingesting Propulsion System for the Common Research Model," PMC 2020 Apr 12.
99. Hu, X.; Qian, Y.; Dong, C.; Zhang, Y.; Wang, C.; Zhuge, W., "Thermal Benefits of a Cooling Guide Vane for an Electrical Machine in an Electric Ducted Fan," Aerospace 2022, 9,583.
100. Alexander Heidebrecht, Klaas Burger, Maurice Hoogreef, Roelof Vos, Askin T. Isikveren & Arvind Gangoli Rao, "Development of a Hydrogen-Powered Fuselage-Mounted BLI Propulsor Add-On For Passenger Aircraft", ICAS 2022
101. Hussain Nouri, Florent Ravelet, Farid Bakir, Christophe Sarraf, "Design and Experimental Validation of a Ducted Counter-rotating Axial-flow Fans System," 28 Aug 2012
102. Xuanyang Hu, Yuping Qian, Bijie Yang, Chaofan Dong, Aerodynamic Design of Cooling 1 Guide For Electrical Machine in 2 Electric Ducted Fan, GTP-22-1505, Journal of Engineering for Gas Turbines and Power. October 20, 2022
103. Tobias Ebus and Markus Dietz, "Small electrically powered contra-rotating turbo fan engines for high-speed aircraft application," AIAA SciTech 2020 Forum
104. Daniel Lawrence Tweedt, "The aerodynamics of a baseline supersonic throughflow fan rotor," Iowa State University Capstones, Theses and Dissertations,1993
105. Durgesh Chandel, John D. Reband, David K. Hall, Thanathepan Balachandran, Student Member, IEEE, Jianqiao Xiao, Student Member, IEEE, Kiruba S. Haran, Fellow, IEEE, Edward M. Greitzer, "Fan and Motor Co-optimization for a Distributed Electric Aircraft Propulsion System," IEEE Transactions On Transportation Electrification, 2022
106. Majid T. Fard, Student Member, IEEE, JiangBiao He, Senior Member, IEEE, Hao Huang, Fellow, IEEE, Yue Cao, Member, IEEE, Aircraft Distributed Electric Propulsion Technologies - A Review, IEEE Transactions on Transportation Electrification, 2022
107. Alan H. Epstein, Aeropropulsion for Commercial Aviation in the Twenty-First Century and Research Directions Needed, AIAA Journal, Vol. 52, No. 5, May 2014
108. Arne Seitz, Oliver Schmitz, Askin T. Isikveren and Mirko Hornung, Bauhaus Luftfahrt e.V., Deutschland, Electrically Powered Propulsion: Comparison and Contrast To Gas Turbines, Deutscher Luft- und Raumfahrtkongress 2012
109. Robert Cameron Bolam, Yuriy Vagapov, Jon Laughton, Alecksey Anuchin, Optimum Performance Determination of Single-Stage and Dual-Stage (Contra-Rotating) Rim Driven Fans for Electric Aircraft, 2020 XI International Conference on Electrical Power Drive Systems (ICEPDS), Saint-Petersburg, Russia, October 04-07, 2020
110. Jonathan Z. Bird, A Review of Electric Aircraft Drivetrain Motor Technology, IEEE Transactions On Magnetics, Vol. 58, No. 2, February 2022
111. Samith Sirimanna, Thanathepan Balachandran, Noah Salk, Jianqiao Xiao, Dongsu Lee, and Kiruba Haran, Electric Propulsors for Zero-Emission Aircraft Partially superconducting machines, IEEE Electrification Magazine, June 2022
112. Durgesh Chandel, John D. Reband, David K. Hall, Thanathepan Balachandran§, Jianqiao Xiao ¶, and Kiruba S. Haran, Edward M. Greitzer, Conceptual Design of Distributed Electrified Boundary Layer Ingesting Propulsors for the CHEETA Aircraft Concept, AIAA Propulsion and Energy 2021 Forum, August 9-11, 2021,
113. Pasquale M. Sforza1, Electric Power Generation Onboard Hypersonic Aircraft, 45th AIAA/ASME/SAE/ASEE Joint Propulsion Conference & Exhibit, 2 - 5 August 2009, Denver, Colorado
114. N.H.M. van den Dungen, Synthesis of an Aircraft Featuring a Ducted-Fan Propulsive Empennage, Master of Science in Aerospace Engineering at the Delft University of Technology, to be defended publicly on Tuesday April 18, 2017 at 13:00h
115. Daniel Weintraub, Jan Koppelberg, Jo Köhler, Peter Jeschke, Ducted fans for hybrid electric propulsion of small aircraft, CEAS Aeronautical Journal (2022) 13:471–485
116. Kenneth A. Brown¹, Jonathan Fleming², Matthew Langford³, and Wing Ng⁴, Development of a Ducted Propulsor for BLI Electric Regional Aircraft - Part I: Aerodynamic Design and Analysis, AIAA, Propulsion and Energy 2019 Forum,
117. B.J.Lee¹, May-Fun Liou², and M. Celestina², Conceptual Design of a Counter-Rotating Fan System for Distributed Boundary Layer Ingesting Propulsion, ISABE-2019-24285
118. W.C. Strack and G. Knip, A.L. Weisbrich, J. Godston, E. Bradley, Technology and Benefits of Aircraft' Counter Rotation Propellers, NASA Technical Memorandum 82983, 1982, 1982 Aerospace Congress and Exposition sponsored by the Society of Automotive E